Trends and variability of sea surface temperature in the Northwest Atlantic from the HadISST1, ERSST, and COBE datasets

John W. Loder, Zeliang Wang, Augustine van der Baaren and Roger Pettipas

Ocean and Ecosystem Sciences Division
Fisheries and Oceans Canada
Bedford Institute of Oceanography
P.O. Box 1006
Dartmouth, Nova Scotia
Canada B2Y 4A2

2013

Canadian Technical Report of
Hydrography and Ocean Sciences 292

Fisheries and Oceans Canada | Pêches et Océans Canada

Canada

Canadian Technical Report of Hydrography and Ocean Sciences

Technical reports contain scientific and technical information of a type that represents a contribution to existing knowledge but which is not normally found in the primary literature. The subject matter is generally related to programs and interests of the Oceans and Science sectors of Fisheries and Oceans Canada.

Technical reports may be cited as full publications. The correct citation appears above the abstract of each report. Each report is abstracted in the data base *Aquatic Sciences and Fisheries Abstracts*.

Technical reports are produced regionally but are numbered nationally. Requests for individual reports will be filled by the issuing establishment listed on the front cover and title page.

Regional and headquarters establishments of Ocean Science and Surveys ceased publication of their various report series as of December 1981. A complete listing of these publications and the last number issued under each title are published in the *Canadian Journal of Fisheries and Aquatic Sciences*, Volume 38: Index to Publications 1981. The current series began with Report Number 1 in January 1982.

Rapport technique canadien sur l'hydrographie et les sciences océaniques

Les rapports techniques contiennent des renseignements scientifiques et techniques qui constituent une contribution aux connaissances actuelles mais que l'on ne trouve pas normalement dans les revues scientifiques. Le sujet est généralement rattaché aux programmes et intérêts des secteurs des Océans et des Sciences de Pêches et Océans Canada.

Les rapports techniques peuvent être cités comme des publications à part entière. Le titre exact figure au-dessus du résumé de chaque rapport. Les rapports techniques sont résumés dans la base de données *Résumés des sciences aquatiques et halieutiques*.

Les rapports techniques sont produits à l'échelon régional, mais numérotés à l'échelon national. Les demandes de rapports seront satisfaites par l'établissement auteur dont le nom figure sur la couverture et la page de titre.

Les établissements de l'ancien secteur des Sciences et Levés océaniques dans les régions et à l'administration centrale ont cessé de publier leurs diverses séries de rapports en décembre 1981. Vous trouverez dans l'index des publications du volume 38 du *Journal canadien des sciences halieutiques et aquatiques*, la liste de ces publications ainsi que le dernier numéro paru dans chaque catégorie. La nouvelle série a commencé avec la publication du rapport numéro 1 en janvier 1982.

Canadian Technical Report of
Hydrography and Ocean Sciences 292

2013

Trends and variability of sea surface temperature in the Northwest Atlantic from the HadISST1, ERSST and COBE datasets

by

John W. Loder, Zeliang Wang, Augustine van der Baaren and Roger Pettipas

Ecosystems and Oceans Science Sector
Maritimes Region
Fisheries and Oceans Canada

Bedford Institute of Oceanography
P. O. Box 1006
Dartmouth, Nova Scotia
Canada B2Y 4A2

© Her Majesty the Queen in Right of Canada, 2013

Cat. No. Fs 97-18/292E ISSN 0711-6764 (print version)

Cat. No. Fs 97-18/292E-PDF ISSN 1488-5417 (on-line version)

Correct Citation for this publication:

Loder, J.W., Z. Wang, A. van der Baaren and R. Pettipas. 2013. Trends and variability of sea surface temperature in the Northwest Atlantic from the HadISST1, ERSST and COBE datasets. Can. Tech.. Rep. Hydrogr. Ocean. Sci. 292: viii + 36 p.

TABLE OF CONTENTS

Table of Contents iii

List of Figures iv

List of Tables vi

Abstract vii

Résumé viii

Section 1: Introduction 1

Section 2: Data and Methods 5

2.1 Historical Interpolated Datasets 5

2.2 DFO Monitoring Datasets 7

Section 3: Results from Annual Mean Data 9

3.1 Trends 9

3.2 Variability of SST in the North Atlantic (NA) 11

3.3 EOF Results for the NW Atlantic (NWA) Sub-Domain 17

Section 4: Results from Summer Mean Data for the North Atlantic 19

4.1 Trends in Summer 19

4.2 Variability of SST in Summer 20

Section 5: SST Variability at DFO Monitoring Sites 24

5.1 Comparison of Gridded SST with DFO Observations 24

5.2 Contributions of Basin-scale Modes to SST Variability at DFO Monitoring Sites 26

Section 6: Summary 31

Acknowledgements 33

References 34

LIST OF FIGURES

Figure 1 Time series of annual-mean SST for three grid squares in each of the Labrador Sea and Scotian Shelf, from HadISST1. The data were provided by the ICES WGPME (O'Brien et al. 2012). 3

Figure 2 Comparison of annual-mean SST from HadISST1 (O'Brien et al. 2012) for three 1^{o}x1^{o} grid squares on the Scotian Shelf (Fig. 1) with those from ERSST (Friedland and Hare 2007) for six 2^{o}x2^{o} grid squares (indicated by the latitude and longitude of their centre position). 4

Figure 3 Map showing locations of the four DFO monitoring sites (green: Bravo, Station 27, Emerald Basin and Prince 5) and the grid squares of the historical datasets (red) used in the comparison. 7

Figure 4 Trends (^{o}C/decade with the zero contour in white) in the various annual-mean datasets for the three periods examined. Note the different scales for the different periods. 9

Figure 5 EOF patterns (in ^{o}C normalized to the peak value) for the annual means for a) 1900-2011, b) 1950-2011 and c) 1979-2011, with the percentage of explained variance indicated in the inset panels. 12

Figure 6a PCs for annual-mean NA SST analyses for 1900-2011. 13

Figure 6b PCs for annual-mean NA SST analyses for 1950-2011. 13

Figure 6c PCs for annual-mean NA SST analyses for 1979-2011. 13

Figure 7 Revised physically-plausible EOF patterns (in ^{o}C normalized to the peak value) for annual-mean SST in the NA for the second (left column) and third (middle column) modes in 1900-2011, and for the third mode (right column) in 1950-2011. For 1900-2011, the original COBE EOF2 has been replaced by the original COBE EOF3, and the original COBE EOF3 replaced by the original COBE EOF4. For 1950-2011, the original COBE EOF3 has been replaced by the original COBE EOF4 (see text). The percentage of variance explained is indicated in the inset panels. 15

Figure 8 Revised physically-plausible PC2s (top panel) and PC3s (middle panel) for 1900-2011, and revised PC3s (right panel) for 1950-2011, for annual-mean NA SST. The original COBE PCs for these modes have been replaced by those for the next highest COBE mode (see text). 16

Figure 9 EOF patterns for the NW Atlantic sub-domain for annual means of SST for 1900-2011, with the percentage of variance explained indicated in the insets. The original COBE EOF2 (which accounted for 21% of the variance) has been rejected and replaced (see text). 18

Figure 10 Revised PCs for the NWA analyses of annual mean SST for 1900-2011. The original PC2 and PC3 for COBE have been replaced by PC3 and PC4, respectively (see text). 18

Figure 11 Trends (°C/decade with the zero contour in white) in the NA in the various summer-mean datasets. Note the different scales for the different periods. 19

Figure 12 EOF patterns for summer means for a) 1900-2011, b) 1950-2011 and c) 1979-2011, with the percentage of variance explained in the inset panels. 21

Figure 13a PCs for the summer NA analyses for 1900-2011. 22

Figure 13b PCs for the summer NA analyses for 1950-2011. 22

Figure 13c PCs for the summer NA analyses for 1979-2011. 22

Figure 14 Time series of annual means of surface temperature at four DFO monitoring sites (black), and of SST in the vicinity of the sites from the three gridded historical datasets (coloured lines). See Section 2.1 for information on the DFO time series. 25

Figure 15 Observed annual-mean anomalies of surface temperature (black circles connected by lines) at the four DFO monitoring sites together with the contributions to local SST variability from the AMO in the three gridded datasets (coloured lines). The AMO contributions are taken from the first mode of the EOF analysis of the de-trended annual means over the NWA during 1900-2011. HD refers to HadISST1, ER to ERSST and CB to COBE. 27

Figure 16 Observed annual mean anomalies of surface temperature (black circles and lines) at the four DFO monitoring sites together with the contributions to historical SST variability from the NAO-linked mode 2 in the three gridded datasets (coloured lines; same abbreviated acronyms as in Figure 15). The second mode is from the EOF analysis of the de-trended annual means over the NWA during 1900-2011, with the revised second mode used for COBE. 28

Figure 17 Observed annual mean anomalies of surface temperature (black circles and lines) at Prince 5 together with the contributions to historical SST variability from the third mode in the three gridded datasets (coloured lines; same abbreviated acronyms as in Table 5). The third mode is from the EOF analysis of the de-trended annual means over the NWA during 1900-2011, with the revised third mode used for COBE. 29

LIST OF TABLES

Table 1 Domains (NA and NWA) used in the trends and EOF analyses, and regions (all) for which trends of the spatially-averaged data are presented (Tables 2 and 3). The regions were approximated by latitude-longitude boxes with the indicated ranges. The Mid-Lat WNA TZ refers to the mid-latitude Western North Atlantic Transition Zone between the subpolar and subtropical gyres (see Brock et al., 2012, for discussion). 6

Table 2 Trends in annual-mean SST (°C/decade) averaged over the whole NA and NWA domains, and over latitude/longitude boxes approximating regions of interest (Table 1), from the three SST datasets (HadISST1 in blue, ERSST in red and COBE in green) and for the three different periods. Trends significant at the 95% confidence level (without consideration of autocorrelation in the time series) are in **boldface**. The average of the trends over the three datasets is shown in black, after the others. The asterisk (*) indicates that the trend is affected by suspicious warming around Greenland in the COBE dataset (prior to 1979), possibly related to sparse data and/or the interpolation scheme. See Table 1 for definitions of the regions. 10

Table 3 Trends in summer SST (°C/decade) averaged over the whole NA and NWA domains, and over latitude/longitude boxes approximating regions of interest, from HadISST1 in blue, ERSST in red and COBE in green) and for the three different periods. Trends significant at the 95% confidence level (without consideration of autocorrelation in the time series) are in **boldface**. The average of the trends over the three datasets is shown in black. The asterisk (*) indicates that the trend is affected by suspicious warming around Greenland in the COBE dataset (prior to 1979). 20

Table 4 Trends in annual-mean upper-ocean temperature (°C/decade) over the entire period of record at the DFO monitoring sites, together with the trends in the annual-mean SST datasets at nearby positions (i.e. of the time series shown in Fig. 14) and the average of the trends (Avg Hist) for these historical datasets. Trends significant at the 95% confidence level (without consideration of autocorrelation in the time series) are in **boldface**. 26

Table 5 Correlation coefficients between the observed upper-ocean annual temperature anomalies from DFO monitoring at four sites in the NWA, and the contributions of the first (AMO-like; left columns), second (NAO-linked; middle columns) and third (right columns) modes from the EOF analyses of the three gridded historical datasets for the NWA domain and the period 1900-2011. Both the DFO and historical dataset indices were de-trended before the computations. Coefficients that are statistically significant at the 95% level are indicated in **boldface**. The datasets are indicated by the abbreviated acronyms HD (HadISST1), ER (ERSST) and CB (COBE). 29

Abstract

Loder, J.W., Z. Wang, A. van der Baaren and R. Pettipas. 2013. Trends and variability of sea surface temperature in the Northwest Atlantic from the HadISST1, ERSST and COBE datasets. Can. Tech. Rep. Hydrogr. Ocean. Sci. 292: viii + 36 p.

Trend and Empirical Orthogonal Function (EOF) analyses of three gridded monthly sea surface temperature (SST) datasets (HadISST1, ERSST and COBE) for the North Atlantic (NA) were carried out for 1900-2011, 1950-2011, and 1979-2011. Analyses were performed for annual and summer means. Comparison of annual-mean time series of the gridded data with time series of upper-ocean temperature from four DFO monitoring sites reveals substantial similarity in the inter-annual to multi-decadal variability at the sites, but also some notable differences in the trends and variability that point to some unresolved data-quality issues in the historical datasets.

All three gridded datasets show positive trends in much of the NA during all three periods, as well as an area south of Greenland with negative trends during 1900-2011 and 1950-2011. However, there are quantitative differences of up to about a factor of two (among the datasets) in the magnitudes of the statistically-significant trends for a particular period, and differences of comparable magnitude between the trends for these two periods for a particular area. In contrast to the trends, there is remarkable similarity among the first, second and third EOF modes of the gridded datasets for 1900-2011 and 1950-2011 after de-trending and screening. The first EOF mode accounts for 31-41% of the variance in annual means for the NW Atlantic (NWA) during 1900-2011 and closely resembles the Atlantic Multi-decadal Oscillation (AMO). The second EOF mode accounts for 11-16% of the variance in the NWA and shows some resemblance to the documented influence of the North Atlantic Oscillation (NAO) on NWA SST, in both spatial and temporal variability, with correlation coefficient values of approximately -0.5 between the Principal Components (PCs) and the winter NAO index. The origin of the third mode, which accounts for 7-12% in the NWA, is less clear, but it appears to be related to variability in the interaction of the NA's subpolar and subtropical gyres.

Résumé

Loder, J.W., Z. Wang, A. van der Baaren et R. Pettipas. 2013. Tendances et variations de la température de la surface de la mer dans l'Atlantique Nord-Ouest selon les ensembles de données HadISST1, ERSST et COBE.. Rapp. tech. can. hydrogr. sci. océan. 292: viii + 36 p.

On a mené, pour les périodes de 1900 à 2011, de 1950 à 2011 et de 1979 à 2011, des analyses des tendances et de la fonction orthogonale empirique (FOE) de trois ensembles de données carroyées sur la température de la surface de la mer mensuelle (HadISST1, ERSST et COBE) dans l'Atlantique Nord. Ces analyses ont été réalisées pour déterminer les moyennes annuelles et estivales. Si l'on compare la série chronologique moyenne annuelle des données carroyées par rapport à la série chronologique de la température de la couche supérieure de l'océan de quatre sites de surveillance de Pêches et Océans Canada, on constate une similarité importante quant à la variation interannuelle à multidécennale aux sites. Toutefois, on observe aussi des différences importantes quant aux tendances et aux variations qui mettent en évidence les problèmes non résolus en ce qui concerne la qualité des données des ensembles historiques.

Les trois ensembles de données carroyées révèlent des tendances positives dans une grande partie de l'Atlantique Nord au cours des trois périodes, ainsi que des tendances négatives dans une région au sud du Groenland pendant les périodes de 1900 à 2011 et de 1950 à 2011. On constate cependant des différences quantitatives jusqu'à environ un facteur de deux (entre les ensembles de données) quant à l'ampleur des tendances significatives sur le plan statistique pour une période particulière période, de même que des différences d'ampleur comparable entre les tendances dans une région particulière au cours de ces deux premières périodes. Par rapport aux tendances, on observe une similarité remarquable entre le premier, le deuxième et le troisième mode de la FOE des ensembles de données carroyées pour les périodes de 1900 à 2011 et de 1950 à 2011, à la suite de la décomposition des tendances et d'analyses. Le premier mode de la FOE représente de 31 à 41 % des écarts des moyennes annuelles dans l'Atlantique Nord-Ouest de 1900 à 2011. De plus, il ressemble beaucoup à l'oscillation atlantique multidécennale (OAM). Le deuxième mode de la FOE, qui représente de 11 à 16 % des écarts observés dans l'Atlantique Nord-Ouest, présente une certaine ressemblance avec l'influence documentée de l'oscillation nord-atlantique sur la température de la surface de la mer de l'Atlantique Nord-Ouest, en ce qui a trait aux variations spatiales et temporelles, avec un coefficient de corrélation d'environ -0,5 entre les principales composantes (PC) et l'indice d'oscillation nord-atlantique en hiver. L'origine du troisième mode, qui représente de 7 à 12 % des écarts observés dans l'Atlantique Nord-Ouest, est moins claire. Néanmoins, ce mode semble être lié aux variations quant à l'interaction des tourbillons subpopulaires et subtropicaux de l'Atlantique Nord.

Section 1 Introduction

Sea surface temperature (SST) is one of the most important variables for ocean climate change and variability studies. With the longest observational records of any ocean variable (e.g. Yasunaka and Hanawa, 2011), it reflects the important coupling between the atmosphere and ocean in the climate system (e.g. Yu and Boer, 2006) and is an indicator of the upper-ocean temperature that affects ocean biogeochemistry and marine ecosystems, marine activities, and coastal human populations.

SST observations are available from observations on vessels, ocean monitoring programs over the past 50-100 years, and satellite observations during the past three decades. Because of diurnal variability and the large vertical temperature gradient near the ocean surface, there are substantial challenges in the interpretation of SST variability in relation to possible aliasing or biases from sampling with different methodologies (e.g. Rayner et al., 2010). In this report, we analyze three global gridded monthly datasets – namely HadISST1 (Rayner et al., 2003), ERSST (Smith et al., 2008) and COBE (Ishii et al., 2005) – for spatial and sub-annual (i.e. at inter-annual and longer time scales) variability in SST in the North Atlantic (NA).

Our focus is the Northwest Atlantic (NWA), in order to provide input to Fisheries and Oceans Canada's (DFO's) Aquatic Climate Change and Adaptation Services Program (ACCASP) for the Atlantic Large Aquatic Basin (LAB) off Canada (Loder et al., 2013). The NWA is one of the most dynamic parts of the world's oceans, with the competing influences of the Labrador Current and Gulf Stream, Arctic Ocean outflows and atmospheric flows from the Arctic and North American continent, and variability in the Atlantic Meridional Overturning Circulation (AMOC) that has one of its primary densification (sinking) regions in the Labrador Sea. Analyses of historical hydrographic profiles have revealed cool fresh ocean conditions in the Scotian Shelf region during the 1960s (e.g. Petrie and Drinkwater, 1993), and cool fresh conditions in the Labrador Sea in the 1980s and early 1990s (e.g. Yashayaev, 2007). In both cases, the anomalous conditions were attributed to persistent winter anomalies of the North Atlantic Oscillation (NAO). In the Labrador Sea case, a direct influence of anomalous atmospheric forcing (positive NAO anomalies) on ocean temperature and salinity was suggested, and in the Scotian Shelf case, the suggestion was an indirect influence from anomalous atmospheric conditions (negative NAO anomalies) and resulting changes in the equatorward extent of the subpolar gyre (and Labrador Current). However, it is not clear that the origin of these and other ocean anomalies are solely related to variability in the NAO (also see Deser et al., 2010, for NAO influences on SST in the NWA).

On larger scales, there is strong multi-decadal variability in SST in the NA (e.g. Deser et al., 2010; Polyakov et al., 2010; Terray, 2012). In particular, the Atlantic Multi-decadal Oscillation (AMO), also referred to as the Atlantic Multi-decadal Variability (AMV; Hakkinen et al., 2011; Ou, 2012), has been identified in spatially-averaged SST (over the NA) with a predominant variation with a period of approximately 60-70 years (Knight et al., 2005; Wang et al., 2012).

There are indications of overall cooling from the late 1950s to the early 1970s and overall warming from the 1980s to the early 2000s. The underlying spatial patterns in both cases point to largest magnitudes in the subpolar NA. Recent analyses of proxy climate variables over the past 8,000 years (Knudsen et al., 2011), and of $\delta^{18}O$ variability in Greenland ice cores together with atmosphere-ocean model simulations over the past millennium (Chylek et al., 2012), suggest intermittent variability in air temperatures similar to the recent AMV in SST. This indicates that the AMV might be related to natural internal variability of the coupled climate system.

There are many suggestions in the literature that the AMO may be related to variability in the AMOC (e.g. Park and Latif, 2010; Medhaug and Furevik, 2011; Drijfhout et al., 2012), multi-decadal variability in the NAO (e.g. Robson et al., 2012), or atmospheric blocking over the northern NA (e.g. Hakkinen et al., 2011). It may be appropriate to think of the AMO, NAO, and AMOC variability as different manifestations (with somewhat differing space and time scales) of coupled atmosphere-ice-ocean variability in/over the NA and adjoining regions (e.g. Arctic and North America via the NAO, and South Atlantic via AMOC variability). These possibilities make it important to understand SST variability in the NWA in relation to larger-scale climate variability, particularly for attribution studies and climate change projections. In particular, the extent to which regional ocean temperature variability (e.g. Labrador Sea and Scotian Shelf as mentioned above) is influenced by, or linked to, the AMO is unclear. Therefore, in this report, we include a comparison of the variability of SST in the three gridded datasets with that in time series of upper-ocean temperature from the DFO AZMP and AZOMP monitoring programs[1].

Friedland and Hare (2007) using ERSST data, and Shearman and Lentz (2010) using ship and shore-based observations, found overall warming and multi-decadal variability in SST along the U.S. east coast. Belkin (2009), using the Hadley SST climatology, found changes of 1.0°C, 0.9°C and 0.2°C during 1982-2006 on the Newfoundland-Labrador Shelf, Scotian Shelf, and northeastern U.S. Shelf, respectively, and suggested that the recent "rapid" warming in the subpolar NA was likely related to NAO variability.

Specific motivation for our analyses stemmed from our initial exploration of annual-mean HadISST1 time series for selected locations (provided by William Li, DFO). Figure 1 shows intriguing patterns with coherent multi-decadal variability at three sites on the Scotian Shelf, including a cool period in the 1960s similar to that found by Petrie and Drinkwater (1993). There is also coherent (but different) decadal-scale variability at three sites across the Labrador Sea. Loder et al. (2012) confirmed different decadal to multi-decadal variability in HadISST1 data in different parts of the Atlantic Canadian shelf/slope region, and found different trends for different time periods in these regions as a result of this variability. Comparison of time series of

[1] Atlantic Zone Monitoring Program (AZMP) and Atlantic Zone Off-shelf Monitoring Program (AZOMP): http://www.bio.gc.ca/science/monitoring-monitorage/index-eng.php

annual means of the ERSST monthly mean data for the Scotian Shelf and Gulf of Maine (provided by Kevin Friedland, NOAA) and HadISST1 annual means for various Scotian Shelf sites (Fig. 2) revealed strong similarity in the variability between the two datasets, but notable differences in the trends. Consequently, we decided to carry out the more in-depth analyses discussed in this report.

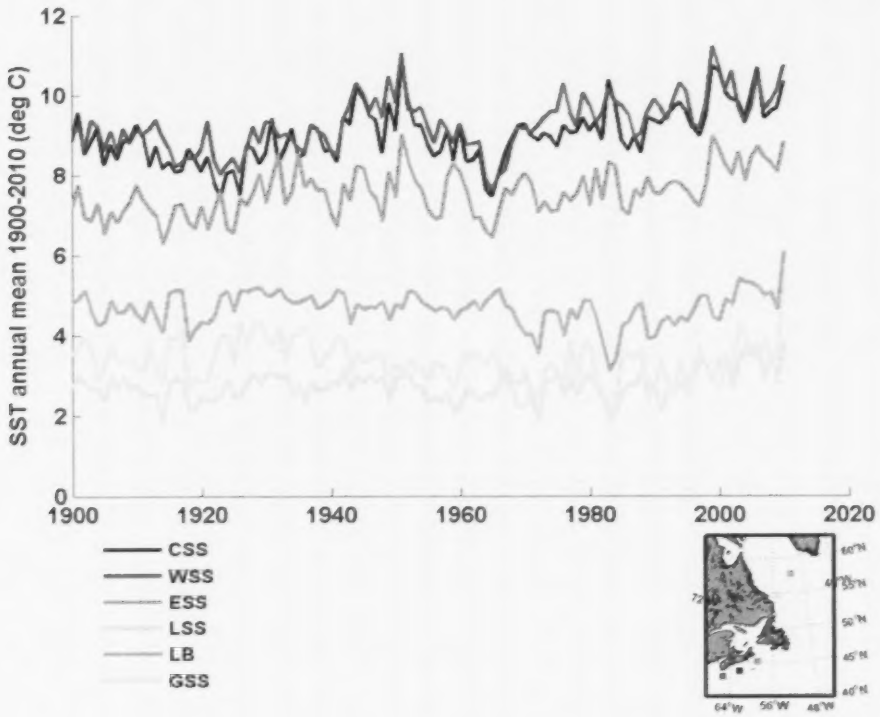

Figure 1 Time series of annual-mean SST for three grid squares in each of the Labrador Sea and Scotian Shelf (lower right panel), from HadISST1. The data were provided by the ICES WGPME (O'Brien et al. 2012).

Our analyses are complementary to ACCASP SST trend analyses for the Atlantic LAB carried out by Galbraith and Larouche (2013) and Hebert (2013) focussed on the Atlantic shelf, using satellite data since 1985 and DFO "Climate" data since 1950, respectively, and to trend analyses of off-shelf upper-ocean temperature in the NWA since 1945 by Han et al. (2013). In particular, Han et al. (2013) also use a version of the COBE historical dataset (Ishii et al., 2006), although for different periods and domains and with additional subsurface data.

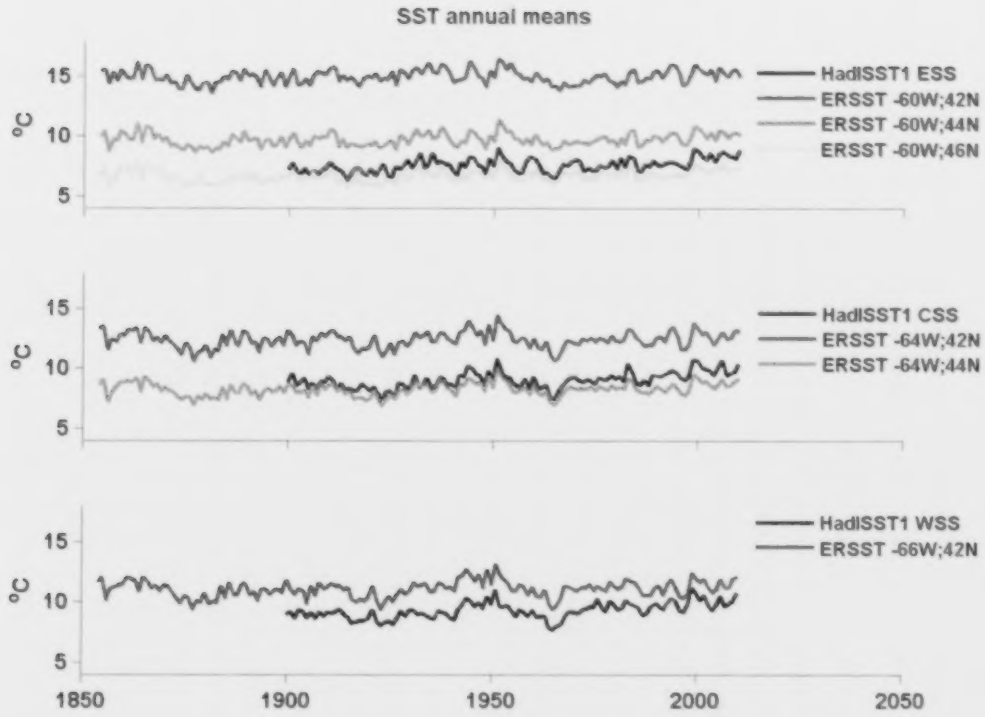

Figure 2 Comparison of annual-mean SST from HadISST1 (O'Brien et al. 2012) for three 1°x1° grid squares on the Scotian Shelf (Fig. 1) with those from ERSST (Friedland and Hare 2007) for six 2°x2° grid squares (indicated by the latitude and longitude of their centre position).

Section 2 of our report describes data and methods used in the analyses. The primary results are presented in Section 3, based on annual means. Results based on summer means are presented in Section 4, and a brief comparison with observations at four DFO monitoring sites is presented in Section 5. The report concludes with a summary in Section 6.

Section 2 Data and Methods

2.1 Historical Interpolated Datasets

The three gridded and interpolated datasets of historical monthly SST are:

- HadISST1 (version 1) which is the United Kingdom Met Office's Hadley Centre Interpolated SST dataset, with 1^{o} x 1^{o} resolution extending back to 1870 (Rayner et al., 2003);
- ERSST (version 3b) which is the United States NOAA's Extended Reconstruction of SST dataset, with 2^{o} x 2^{o} resolution extending back to 1854 (Smith et al., 2008); and
- COBE SST which is the Japanese Meteorological Agency's Centennial in-situ Observation-Based Estimates of variability of SST, with 1^{o} x 1^{o} resolution extending back to 1891 (Ishii et al., 2005).

Data quality, especially during the early part of the records and in remote and/or ice-covered regions, is an issue with these datasets (e.g. Yasunaka and Hanawa, 2011) so that the results in some periods and areas need to be interpreted with caution. These datasets were derived from differing combinations of ICOADS (International Comprehensive Ocean-Atmosphere Data Set) and other observations, using different methodologies for quality control and interpolation. HadISST1 used reduced-space optimal interpolation, ERSST used Empirical Orthogonal Functions (EOFs), and COBE an optimal interpolation scheme.

Two derived datasets for inter-annual and longer-term variability studies of SST in the "North Atlantic (NA)" have been computed from each of the source datasets: annual means computed from the monthly means for all months, and summer means computed from the monthly means for July, August, and September. For this purpose, the NA is defined as the region in the latitude and longitude ranges that are listed in Table 1, with the Mediterranean excluded. Since ERSST and COBE have estimated monthly SST values (often -1.8°C) in ice-covered regions such as Baffin Bay and the Greenland and Labrador Shelves, their values were used for the entire domain. In contrast, HadISST1 has missing or dubious data in some ice-covered areas in which case we omitted those grid squares from our annual-mean analyses. We analyzed the summer means to provide increased spatial coverage in these areas, and to obtain an indication of the seasonal dependence.

Trend and EOF analyses were carried out on each dataset for the NA domain, for three periods: 1900-2011 in order to provide a century-scale view; 1950-2011 in order to examine variability in the post-war era with more comprehensive ocean sampling; and 1979-2011 in order to examine recent variability during the high-resolution satellite era. We used standard linear regression techniques for the trend analysis. We performed the EOF analyses with and without prior de-trending but, after discussing the trend analysis, we only report the EOF results based on de-trended datasets.

Table 1 Domains (NA and NWA) used in the trends and EOF analyses, and regions (all) for which trends of the spatially-averaged data are presented (Tables 2 and 3). The regions were approximated by latitude-longitude boxes with the indicated ranges. The Mid-Lat WNA TZ refers to the mid-latitude Western North Atlantic Transition Zone between the subpolar and subtropical gyres (see Brock et al., 2012, for discussion).

Domain or Region	Abbreviation	Latitude (°N)	Longitude (°W)
North Atlantic	NA	6.5 - 74.5	-29.5 - 100.5
Northwest Atlantic	NWA	30.5 - 74.5	20.5 - 100.5
Labrador Sea/Shelf	LSS	52 - 62	48 - 56
Newfoundland Shelf/Slope	NSS	44 - 52	46 - 56
Mid-Lat WNA TZ: Shelf	MLTZ-S	42 - 50	56 - 70
Mid-Lat WNA TZ: Off-Shelf	MLTZ-OS	34 - 42	52 - 74
Newfoundland Basin	NB	40 - 46	40 - 46
Flemish Cap	FC	46 - 50	42 - 46
Northwest Corner	NWC	50 - 54	36 - 46
South Greenland	SG	54 - 60	40 - 48

The EOF values for each analysis were normalized by dividing the values for all grid points in each domain by the maximum absolute value of the anomaly for any point in the domain. For consistency, the corresponding Principal Component (PC) time series for each analysis were normalized by multiplying each of its values by the same maximum EOF value that was used to normalize the corresponding EOF pattern.

Results are presented first for the annual-mean datasets and then for the summer means. For the annual means, EOF results for a "Northwest Atlantic (NWA)" sub-domain (Table 1) are also displayed, in order to examine the sensitivity of the EOF results to the size of the domain considered and provide magnified displays for the ACCASP area of interest.

To provide an indication of the magnitude of the trends in various sub-regions of interest, the trends are presented for spatially-averaged data from the ten sub-regions indicated in Table 1. The statistical significance of the trends at the 95% confidence level is indicated, with the number of degrees of freedom estimated from the number of data points. Because there appears to be some autocorrelation in the time series, the statistical significance is probably overestimated.

2.2 DFO Monitoring Datasets

We compared time series of the annual means of upper-ocean temperature from four DFO monitoring sites (Fig. 3) with the gridded SST data. Three of the DFO temperature time series were for the upper few meters from AZMP:

- observations since the 1920s at Prince 5 in Passamaquoddy Bay in the outer Bay of Fundy, collected by DFO's St. Andrews Biological Station;
- observations since the 1940s in Emerald Basin on the Scotian Shelf off Halifax, primarily collected by DFO's Bedford Institute of Oceanography (BIO);
- observations since the 1940s at Station 27 on the Grand Bank off St. John's, primarily collected by DFO's Northwest Atlantic Fisheries Centre (NAFC).

For recent reports on these observed data, see Hebert et al. (2012) and Colbourne et al. (2012).

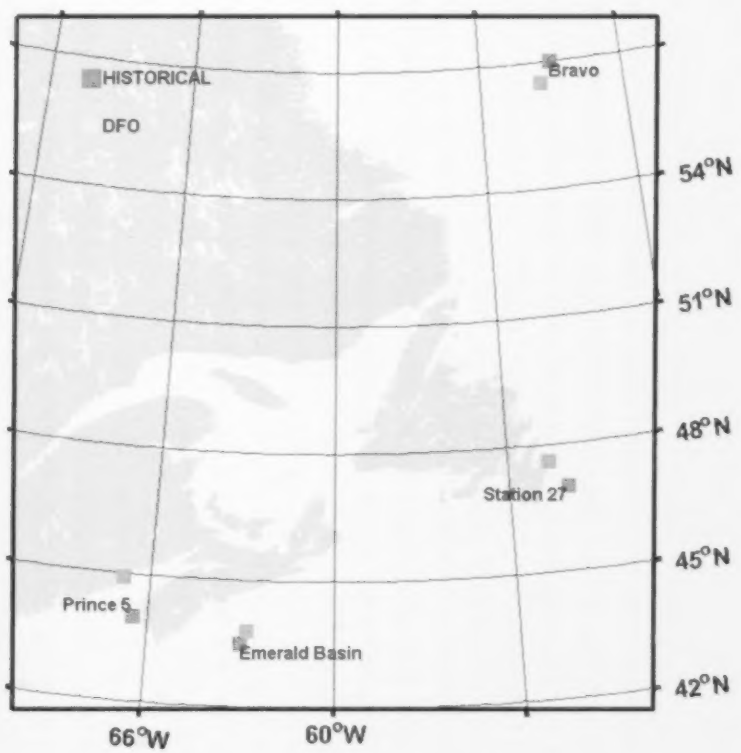

Figure 3 Map showing locations of the four DFO monitoring sites (green: Bravo, Station 27, Emerald Basin and Prince 5) and the grid squares of the historical datasets (red) used in the comparison.

The fourth DFO time series, from AZOMP provided by Igor Yashayaev (BIO) for the 10-30 m depth interval[2] in the central Labrador Sea, was constructed from data collected in the vicinity of the former Ocean Weather Ship (OWS) Bravo, primarily by the OWS and BIO. This time series used data for most years since 1948 and a few earlier ones. For a recent report, see Yashayaev (2007) or Yashayaev and Greenan (2012).

[2] An interval that does not include the near-surface region was purposely chosen to avoid spurious variations related to seasonal changes and different depths below the surface in the sampling.

Section 3 Results from Annual Mean Data

3.1 Trends

The spatial patterns and magnitudes of the trends from the three historical datasets during the different periods are shown in Figure 4 for the NA, and trends of the spatially-averaged data in regions of interest (Table 1) are shown in Table 2 together with an indication of their statistical significance. The trends from the different datasets are generally similar for particular periods in terms of large-scale patterns, but substantial differences do exist, particularly for 1900-2011, and on smaller scales. Some of the differences among the source datasets are present in multiple periods, while others occur primarily in a particular period. In the NWA, off eastern Canada, there are significant differences in the trends from the different datasets in all three periods, making firm conclusions regarding the magnitude of the trends difficult. The averages of the trends from the three datasets are included in Table 2 to provide a rough indication of the magnitude in each period in each region.

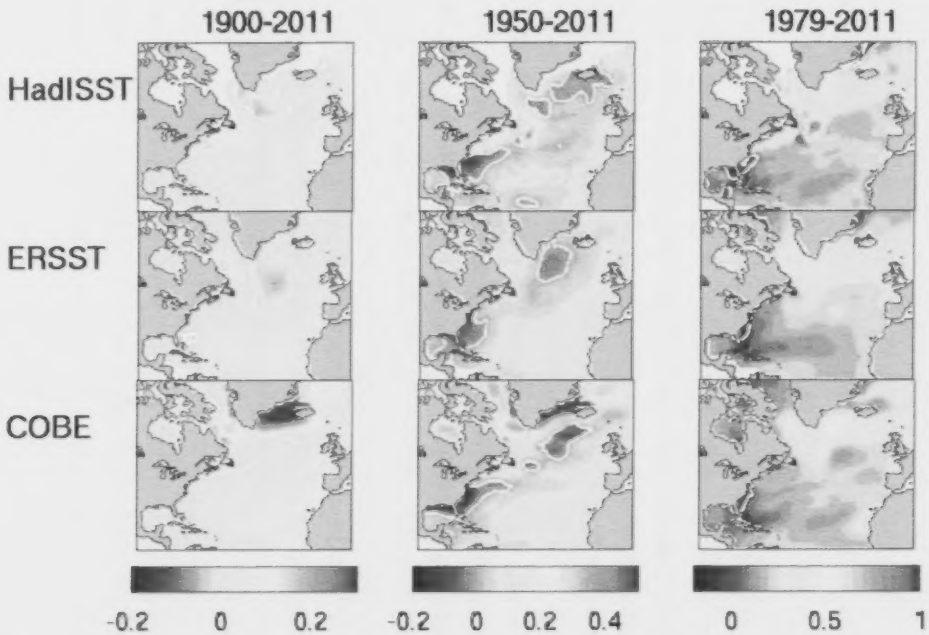

Figure 4 Trends (°C/decade with the zero contour in white) in the various annual-mean datasets for the three periods examined. Note the different scales for the different periods.

Overall, there is broad-scale warming in all three periods and datasets, but not in all areas. The warming trends are largest during 1979-2011, and the trends during this period are more consistent across the datasets than during 1900-2011 and 1950-2011. This is consistent with better data coverage and accelerated global warming during the past few decades.

During 1900-2011, there is warming of 0.05 to 0.1°C/decade over most of the NA in all three datasets, but there is also as an area of cooling or reduced warming south of Greenland, extending into the off-shelf waters off southern Labrador and Newfoundland (Fig. 4). The most noticeable anomaly among the datasets is the strong warming immediately adjacent to Greenland in COBE which is suspect. Because of the areas of cooling or reduced warming in the NWA, the warming trend for the overall NA is only 0.03°C/decade in HadISST1 and 0.05°C/decade in ERSST. There is warming on the Atlantic Canadian shelf/slope in all three datasets but differences in the pattern of its magnitude. The qualitative differences in the trend magnitudes apparent in the HadISST1 and ERSST time series on the Scotian Shelf in Figure 2 are present in the trends in Table 2 for the shelf portion of the mid-latitude transition zone (MLTZ-S), confirming that these differences are shelf-wide rather than local anomalies. The weaker century-scale trend apparent in Figure 1 for the Labrador Sea, compared to the Scotian Shelf, in HadISST1 is clearly present in Table 2 (MLTZ-S versus LSS) for HadISST1, but not for ERSST and COBE. Trends for the Atlantic shelf/slope regions (LSS, NSS, MLTZ-S, and FC) vary widely across regions and datasets, ranging from 0.01 to 0.1°C/decade. Average (across datasets) values are 0.06-0.08°C/decade for LSS, NSS, and MLTZ-S, and 0.03°C/decade for FC.

Table 2 Trends in annual-mean SST (°C/decade) averaged over the whole NA and NWA domains, and over latitude/longitude boxes approximating regions of interest (Table 1), from the three SST datasets (HadISST1 in blue, ERSST in red and COBE in green) and for the three different periods. Trends significant at the 95% confidence level (without consideration of autocorrelation in the time series) are in **boldface**. The average of the trends over the three datasets is shown in black, after the others. The asterisk (*) indicates that the trend is affected by suspicious warming around Greenland in the COBE dataset (prior to 1979), possibly related to sparse data and/or the interpolation scheme. See Table 1 for definitions of the regions.

Region	1900-2011	1950-2011	1979-2011
NA	**0.03** / 0.05 / 0.07* / 0.05	0.01 / 0.07 / 0.10* / 0.06	**0.26** / 0.24 / 0.21 / 0.24
NWA	-0.01 / 0.04 / 0.07* / 0.04	-0.02 / 0.06 / 0.11* / 0.05	**0.33** / 0.29 / 0.23 / 0.28
LSS	0.02 / 0.06 / 0.10 / 0.06	**0.10** / 0.09 / 0.20 / 0.13	**0.42** / 0.51 / 0.39 / 0.44
NSS	**0.01** / 0.05 / 0.06 / 0.04	**0.13**/ 0.06 / 0.11 / 0.10	**0.33** / 0.32 / 0.26 / 0.30
MLTZ-S	**0.11** / 0.05 / 0.09 / 0.08	**0.14** / 0.07 / 0.15 / 0.12	**0.25** / 0.21 / 0.17 / 0.21
MLTZ-OS	**0.08** / 0.04 / 0.05 / 0.06	**0.06** / 0.03 / -0.00 / 0.03	**0.22** / 0.15 / 0.15 / 0.17
NB	**0.06** / 0.00 / 0.03 / 0.03	**0.15** / 0.03 / 0.03 / 0.07	**0.37** / 0.26 / 0.23 / 0.29
FC	**0.06** / 0.01 / 0.01 / 0.03	**0.23** / 0.01 / -0.00 / 0.08	**0.74** / 0.35 / 0.34 / 0.48
NWC	-0.01 / -0.01 / 0.03 / 0.00	0.04 / 0.01 / 0.04 / 0.03	**0.38** / 0.38 / 0.35 / 0.37
SG	-0.01 / -0.00 / **0.08*** / 0.02	0.03 / 0.03 / **0.15*** / 0.07	**0.37** / 0.45 / 0.34 / 0.39

During 1950-2011, the warming rates are larger in most areas and datasets. The suspect warming immediately adjacent to Greenland in COBE is again present. There is, again, warming over the Atlantic Canadian shelf/slope in all three datasets, but with different patterns and magnitudes, and, again, offshore areas of cooling south of Greenland. There are also areas of cooling off the southeastern (SE) U.S. extending north of Cape Hatteras in all three datasets, such that the areas of warming are less widespread. As a result, the warming trend for the overall NA is only slightly increased in ERSST and COBE (compared to 1900-2011), and actually decreased in HadISST1 (the reduced domain of the analyzed HadISST1 data for 1900-2011 and 1950-2011 may also be a factor in their NA and NWA trends in Table 2 differing from those for ERSST and COBE). Average trends (across datasets) for the Atlantic shelf/slope regions are in the range of 0.08 to 0.13°C/decade for 1950-2011. It is noteworthy that, in the offshore FC and NB regions, the HadISST1 data show strong warming of ~0.2°C/decade, while there is little warming in the other datasets suggesting that the HadISST1 trend may not be reliable. However, this feature could be a local indication of a northward creep of the Gulf Stream (Wu et al., 2012).

During 1979-2011, there is a common pattern of widespread warming over almost all the NA and a small area of cooling off the SE U.S. in all three datasets. There is no anomalous warming in COBE immediately adjacent to Greenland. There is a clear indication in all three datasets of greater warming in the subpolar gyre, with peak magnitude of ~0.5°C/decade (Fig. 4). The average (across datasets) trend for the overall NA is 0.24°C/decade, and those for the Atlantic shelf/slope regions are 0.4, 0.3, 0.2 and 0.5°C/decade, for LSS, NSS, MLTZ-S and FC, respectively. These increased warming rates in recent decades probably, in part, reflect anthropogenic global warming but they also include a contribution from natural variability associated with the AMO (see next subsection).

3.2 Variability of SST in the North Atlantic (NA)

The EOF patterns for the NA from the de-trended annual means for the three periods are shown in Figure 5, and the PC time series for the EOFs are shown in Figure 6.

The patterns of the EOF1s (Fig. 5a) show considerable similarity. There are positive anomalies over most of the domain and strong positive anomalies in the subpolar gyre (including off Atlantic Canada south to the Scotian Shelf) and in the eastern equatorial NA. There are weak anomalies in the subtropical gyre in the western NA and in some high latitude areas (>65°N). This first mode accounts for 30% or more of the variance in all three periods and all datasets, with the exception of only 26% in COBE during 1900-2011 (but see below). The patterns for 1900-2011 and 1950-2011 are also similar to those for the AMO in Knight et al. (2005) and Wang et al. (2012) (see Fig. 1 in each).

The PC1s (Fig. 6) for the different datasets are similar to each other, including a prominent multi-decadal variation that closely resembles the AMO index (see Fig. 1 in each of Knight et al.,

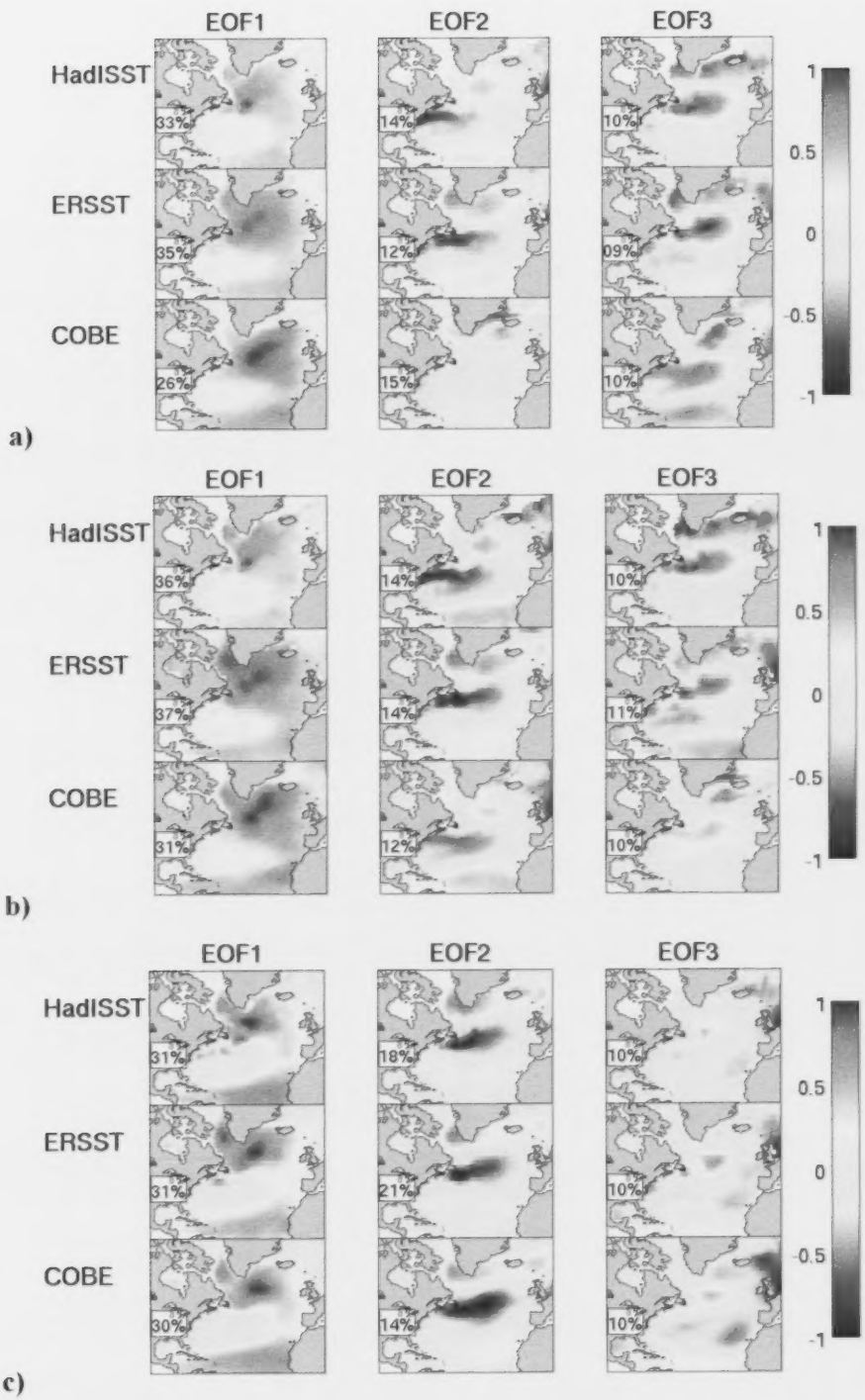

Figure 5 EOF patterns (in °C normalized to the peak value) for the annual means for a) 1900-2011, b) 1950-2011 and c) 1979-2011, with the percentage of explained variance indicated in the inset panels.

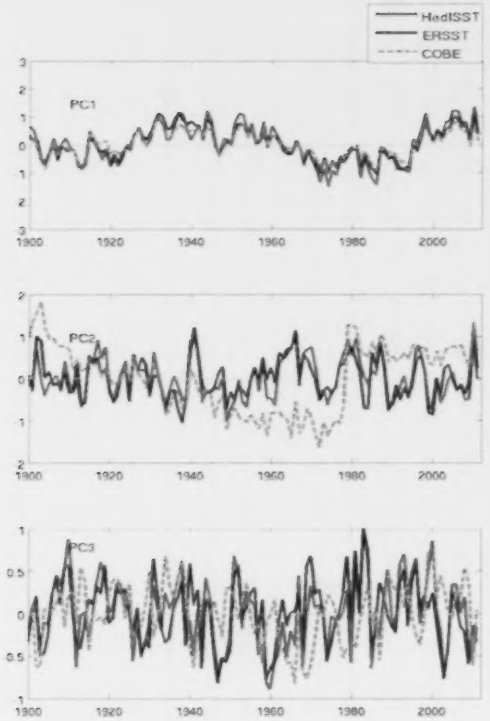

Figure 6a PCs for annual-mean NA SST analyses for 1900-2011.

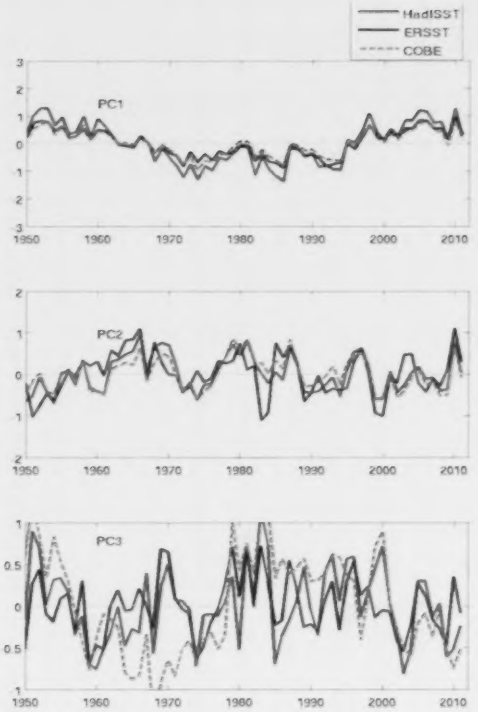

Figure 6b PCs for annual-mean NA SST analyses for 1950-2011.

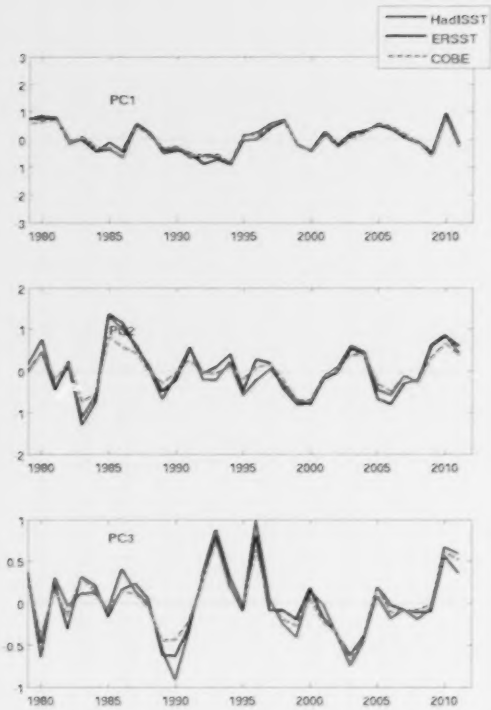

Figure 6c PCs for annual-mean NA SST analyses for 1979-2011.

2005, and Wang et al., 2012). This variation shows a prolonged maximum from the 1930s to the 1950s, a prolonged minimum from the mid-1970s to the early 1990s, and a maximum from the late 1990s to present (see the PC1 panels for 1900-2011 and 1950-2011). Since EOF1 accounts for more than twice as much variance as any other EOF during 1900-2011 and 1950-2011, it can be considered to be the predominant mode of SST variability in the NA during the past century on decadal to multi-decadal time scales. The peak (local) range of this multi-decadal variation is about 2°C (compared to the range of ~0.5°C for the basin-averaged AMO). The correlation coefficients between the AMO index taken from the Global Climate Observing System[3] and then de-trended, and the PC1s from HadISST1, ERSST, and COBE for 1900-2011 are 0.95, 0.92, and 0.91, respectively. Considering these correlations and the similarities of the EOF1 spatial patterns to the corresponding AMO features in Knight et al. (2005) and Wang et al. (2012), it can be argued that the EOF1 patterns and multi-decadal PC1 time variation in Figures 5 and 6, respectively, are credible representations of the AMO.

With the interpretation that EOF1 represents the AMO, comments can be made regarding the contributions of the AMO to SST variability in the NWA. The amplitude of the AMO is largest in a broad area across the northern NA, in the latitude range 40-65°N, with greatest magnitude in the general area of the North Atlantic Current, northeast of Flemish Cap. This suggests that the AMO may be related to gyre-gyre interactions in this region. The broad area of relatively-large AMO amplitude extends west of the Grand Bank (albeit with reduced magnitude) into the Scotian Shelf/Slope region which distinguishes this mode from the NAO-forced variation in ocean temperature that has opposite phases in the subpolar gyre and west of the Grand Bank (Petrie, 2007; Deser et al., 2010). The PC1 variation indicates that EOF1 contributed towards below-average SSTs in the subpolar gyre and its extension to the Scotian Shelf/Slope between the mid-1970s and early 1990s, and towards above-average SSTs in this region since the mid-1990s. The EOF1 pattern suggests that the AMO has a weaker influence on SST southwest of the Scotian Shelf and particularly in the western part of the subtropical gyre off the eastern U.S.

The EOF2s (Fig. 5) generally show a quad-pole pattern that is somewhat similar across the datasets and periods, with the exception of COBE during 1900-2011. The PC2 variations are also similar for the different datasets and periods (Fig. 6), except for COBE during 1900-2011. Closer examination indicates that PC2 for COBE during 1900-2011 (Fig. 6a) shows an abrupt shift in the late 1970s that is neither present in the PC2s from the other two datasets nor in the COBE PC2 for 1950-2011 (Fig. 6b), and that the COBE PC2 and EOF2 for 1979-2011 are highly similar to the PC2s and EOF2s for the other two datasets (Fig. 6c). The abrupt shift in the COBE 1900-2011 PC2 is of questionable physical plausibility, while the similarity of the 1979-2011 PC2s across the datasets points to increased reliability of all three datasets since the late 1970s. If the second 1900-2011 COBE mode in Figures 5 and 6 is taken to be an artifact of degraded COBE data and hence rejected from further interpretation, and the original third 1900-

[3] Working Group on Surface Pressure of the Global Climate Observing System (GCOS); see www.esrl.noaa.gov/psd/gcos_wgsp/Timeseries/AMO/

2011 COBE mode is adopted as the physically-plausible second 1900-2011 mode, then there is remarkable similarity among this revised set of 1900-2011 EOF2s (Fig. 7) and PC2s (Fig. 8). The quad-polar pattern is now present in EOF2 of all three datasets during both 1900-2011 and 1950-2011, and the PC2s for 1900-2011 are highly correlated like those for 1950-2011. The revised EOF2s account for 10-21% of the variance in the different datasets and periods.

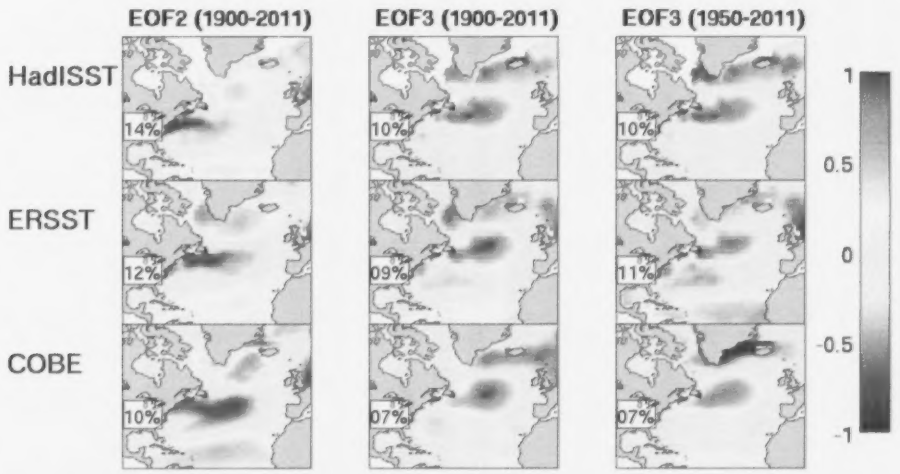

Figure 7 Revised physically-plausible EOF patterns (in °C normalized to the peak value) for annual-mean SST in the NA for the second (left column) and third (middle column) modes in 1900-2011, and for the third mode (right column) in 1950-2011. For 1900-2011, the original COBE EOF2 has been replaced by the original COBE EOF3, and the original COBE EOF3 replaced by the original COBE EOF4. For 1950-2011, the original COBE EOF3 has been replaced by the original COBE EOF4 (see text). The percentage of variance explained is indicated in the inset panels.

Similar to the issue with the original second 1900-2011 COBE mode, the EOF pattern (Fig. 5b) and PC time series (Fig. 6b) for the original third COBE mode for 1950-2011 indicate a suspect enhanced amplitude close to Greenland and anomalous temporal variability, respectively. If this third 1950-2011 COBE mode is also taken to be an artifact of degraded COBE data and rejected from further interpretation, and the original fourth 1950-2011 COBE mode is adopted as the physically-plausible third 1950-2011 COBE mode, then there is also now remarkable similarity among the EOF3s (Figs. 5 and 7) and the PC3s (Figs. 6 and 8). The revised EOF3s now account for 7-11% of the variance in the various cases. Henceforth in this report, we adopt these revisions to the second and third COBE modes for the NA during 1900-2011 and 1950-2011.

In the western NA, the predominant feature of the revised EOF2s is a di-pole structure between the subpolar region to the north and east of the Grand Bank, and the gyre-gyre "transition zone" on and west of the Bank. This out-of-phase temperature pattern, together with the positive PC2 values during the 1960s, are reminiscent of the extension of relatively-cool subpolar water west of the Grand Bank associated with a period of negative NAO (and subpolar gyre relaxation) in the 1960s, at a time when the temperature north of the Bank was above average (Petrie and

Drinkwater, 1993; Deser et al., 2010). The correlation coefficients between the de-trended winter NAO index from GCOS[4] and the PC2s for HadISST1, ERSST and COBE for 1900-2011 are -0.52, -0.48, and -0.46, respectively. These correlations provide some support for previous suggestions that periods of negative NAO result in cooling west of the Grand Bank (Petrie and Drinkwater, 1993; Petrie, 2007) and of positive NAO result in cooling in the Labrador Sea (Yashayaev, 2007). However, the modest values of these coefficients indicate that the NAO is not the only factor contributing to the basin-scale EOF2 mode. The PC2s have more decadal-scale and multi-year variability than the PC1s, consistent with a more complex origin for EOF2.

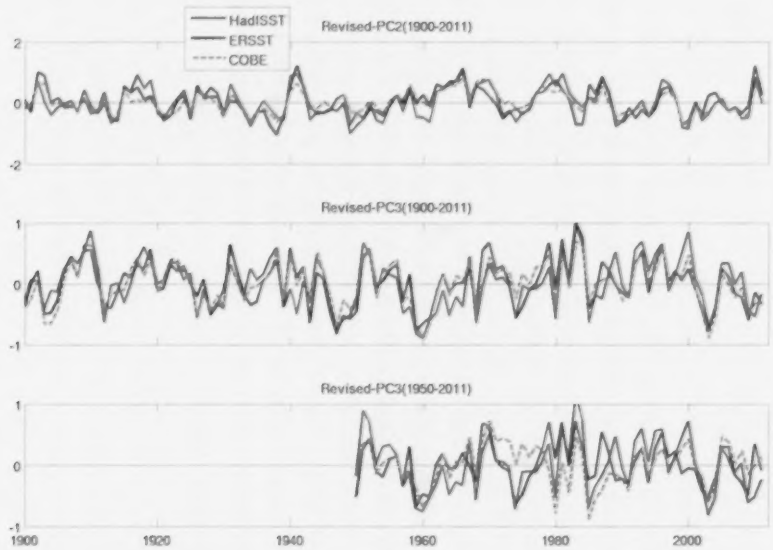

Figure 8 Revised physically-plausible PC2s (top panel) and PC3s (middle panel) for 1900-2011, and revised PC3s (bottom panel) for 1950-2011, for annual-mean NA SST. The original COBE PCs for these modes have been replaced by those for the next highest COBE mode (see text).

The revised EOF3s are generally dominated by a tri-pole pattern. The largest amplitudes are in a zonal band extending eastward from the Grand Bank region and expand latitudinally in the 40-55°W region. Weaker amplitudes are in zonal bands to the north (including the Labrador Sea) and south in the 20-40°N range. During 1900-2011 and 1950-2011, the boundary area where the mode changes sign (between the southern and mid-latitude poles) generally lies near the Gulf of Maine and south of the Grand Bank, whereas that between the subpolar and subtropical poles of EOF2 lies over or north of the Grand Bank. This raises the question of whether this mode is additionally or alternatively connected with previously-described variability in the extension of subpolar water west of the Grand Bank (e.g. Petrie, 2007). The PC3s have substantial decadal-scale and multi-year variability (like the PC2s), as well as notable inter-annual variability (more than the PC2s). The correlation coefficients between the 1900-2011 PC3s and the de-trended

[4] NAO index from GCOS: www.esrl.noaa.gov/psd/gcos_wgsp/Timeseries/NAO/

winter NAO index have magnitudes <0.2, indicating that the winter NAO is not a primary factor in this mode. The interpretation and origin of this EOF are unclear at this point, beyond the peak amplitude east of the Grand Bank indicating that the mode could be related to gyre-gyre interaction associated with the North Atlantic Current. Support for this conjecture comes from correlation coefficients of -0.16, -0.42, and -0.32 between the 1950-2011 PC3s (for HadISST1, ERSST and COBE, respectively) and the sea level difference between Bermuda and Bravo in a recent hindcast simulation of the NA during 1958-2004 (Wang et al., 2013), and coefficients of 0.35, 0.48 and 0.32 with the curl of the wind stress over the NA during this period.

3.3 EOF Results for the NW Atlantic (NWA) Sub-Domain

Trends for the NWA sub-domain are the same as those for the whole NA domain (Fig. 3, Table 2), so we will not repeat them in this subsection. Figures 9 and 10 show results from EOF analyses of de-trended SST for 1900-2011 for the NWA. Similar to the results for the NA domain, the original second COBE mode appeared to be spurious, so the COBE EOF2 and PC2 in these figures have been replaced by the original EOF3 and PC3, respectively. Also, the original COBE EOF3 and PC3 have been replaced by the original EOF4 and PC4, respectively.

There is a strong resemblance among the revised EOF patterns for the NWA for a particular mode (Fig. 9), and to those in Figures 5a (EOF1) and 7 (revised EOF2s and EOF3s) for the NA. The percentage of variance explained is at least slightly higher in all cases than for the NA, with the exception of COBE EOF3 where it is the same. About 40% of the variance is explained by the EOF1s from HadISST1 and ERSST, and 30% by COBE EOF1. The lower percentage for COBE can be explained by the presence in the dataset of the suspect original mode 2 which accounted for 21% of the variance. The revised NWA PCs for a particular mode (Fig. 10) are also closely similar to those in Figures 6a (PC1s) and 8 (revised PC2s and PC3s) for the NA.

The similarities in the EOFs and PCs for the NA and NWA indicate that the NA results for the NWA are not sensitive to domain size and that SST variability in the NWA is associated with larger-scale modes of variability in the NA. The AMO-like first mode has peak amplitudes (Fig. 9) in a broad area east and northeast of Flemish Cap and has the same phase from the Labrador Sea to the Gulf of Maine (with the qualification that its amplitude is weak in the Gulf of Maine in HadISST1). The NAO-linked second mode has a different sign north of the Grand Bank than on and west of the Bank, and has peak amplitudes in the Labrador and/or Irminger Seas and (of opposite phase) in the Gulf Stream and/or the Slope Water region to its north. A weak signature resembling the Labrador Current east of the Grand Bank can be seen in the HadISST1 and ERSST EOF2s. The EOF3s have a clear centre-of-action northeast of the Grand Bank and Flemish Pass, that widens eastward from St. John's, There is a weaker pole of opposite sign extending offshore from the coast between Cape Hatteras and southwestern Nova Scotia.

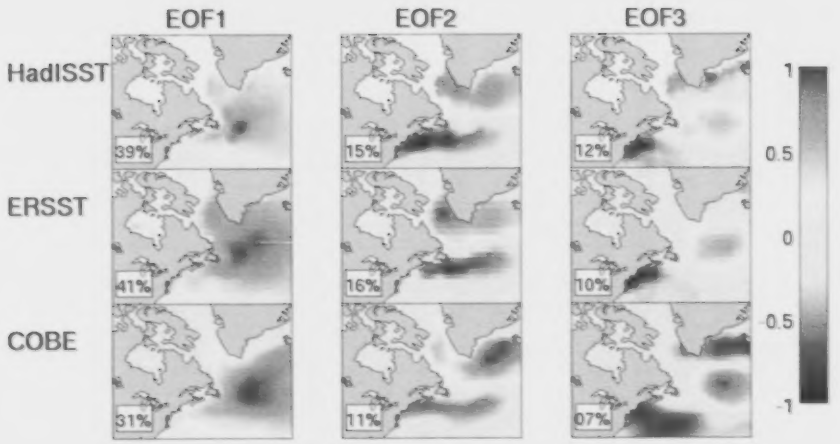

Figure 9 EOF patterns for the NW Atlantic sub-domain for annual means of SST for 1900-2011, with the percentage of variance explained indicated in the inset panels. The original COBE EOF2 (which accounted for 21% of the variance) has been rejected and replaced (see text).

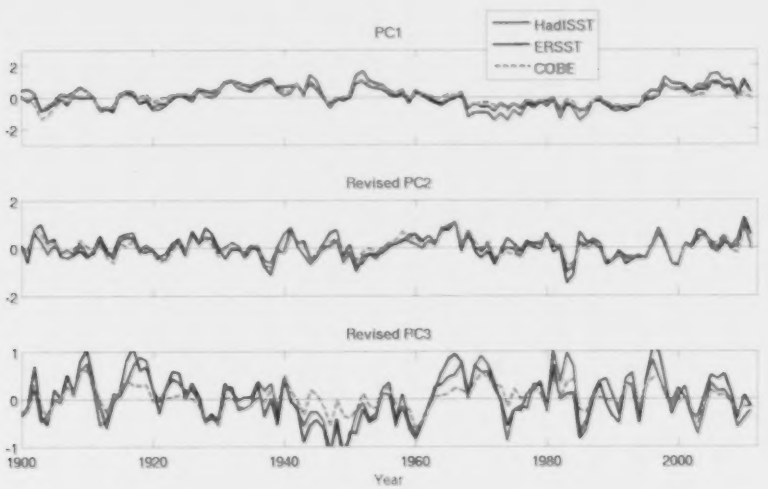

Figure 10 Revised PCs for the NWA analyses of annual mean SST for 1900-2011. The original PC2 and PC3 for COBE have been replaced by PC3 and PC4, respectively (see text).

Section 4 Results from Summer Mean Data for the North Atlantic

4.1 Trends in Summer

The trend and EOF analyses are repeated here for the summer (July-Sept) SST means because there is generally better data coverage in summer such that issues related to data quality in sea ice areas will not be present. The patterns of the summer trends (Fig. 11) are generally similar to those from the annual means, but the trends are generally more positive with smaller areas of negative values in HadISST1 in particular. Table 3 lists the summer trends for spatially-averaged SST in the same regions of interest as in Tables 1 and 2. There is generally stronger warming in all the regions in summer (than in the annual means), that is consistent with expectations for atmosphere-forced warming and shallower ocean mixed layers in summer.

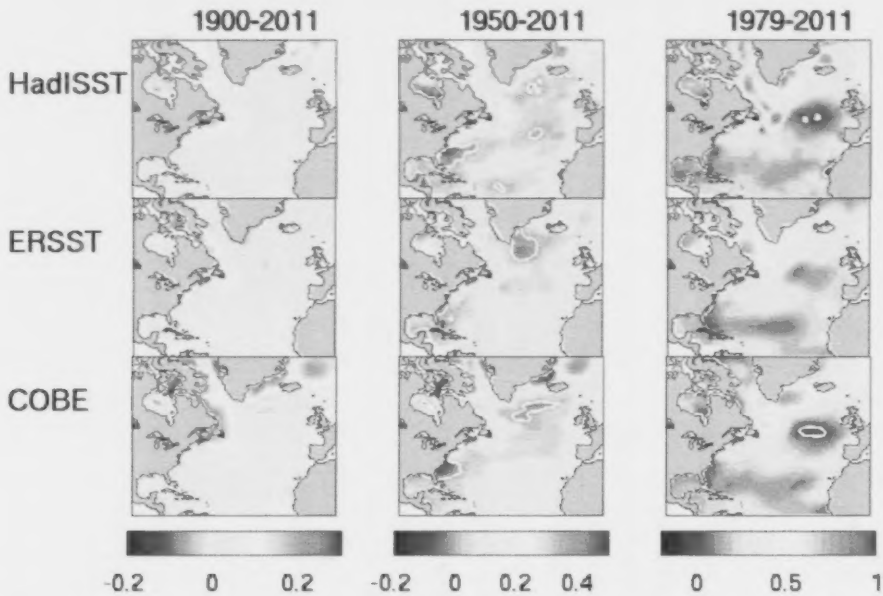

Figure 11 Trends (°C/decade with the zero contour in white) in the NA in the various summer-mean datasets. Note the different scales for the different periods.

For a particular period, discrepancies remain in the detailed structure and magnitude of the trends from the different datasets in the NWA. There is still suspect anomalous warming immediately adjacent to southern Greenland in COBE for 1900-2011 and, to a lesser degree, for 1950-2011. The area of annual-mean cooling farther offshore, south of Greenland, during 1900-2011 and 1950-2011, has largely disappeared from the summer HadISST1 trends, but not from the ERSST and COBE ones. In HadISST1, there is a notable summer warming trend on the Labrador Shelf/Slope that was excluded from the annual-mean analyses (due to seasonal ice cover). This warming is similar to that in ERSST and COBE for 1900-2011, but there are significant differences in the detailed structure and magnitudes. The warming trends for the overall NA during 1900-2011 have increased from 0.03 and 0.05°C/decade for the HadISST1 and ERSST

annual means, respectively, to 0.05 and 0.07°C/decade for the summer means. For the NWA, they have increased from -0.01 and 0.04°C/decade for the annual means to 0.13 and 0.10°C/decade for the summer means. There is also an increase in the Atlantic Canadian shelf/slope regions (LSS, NSS, MLTZ-S, FC).

Table 3 Trends in summer SST (°C/decade) averaged over the whole NA and NWA domains, and over latitude/longitude boxes approximating regions of interest, from HadISST1 in blue, ERSST in red and COBE in green, and for the three different periods. Trends significant at the 95% confidence level (without consideration of autocorrelation in the time series) are in **boldface**. The average of the trends over the three datasets is shown in black. The asterisk (*) indicates that the trend is affected by suspicious warming around Greenland in the COBE dataset (prior to 1979).

Region	1900-2011	1950-2011	1979-2011
NA	**0.05** / **0.07** / **0.09*** / **0.07**	**0.09** / **0.10** / **0.13*** / **0.11**	**0.27** / **0.30** / **0.26** / **0.27**
NWA	**0.08** / **0.07** / **0.10*** / **0.09**	**0.13** / **0.10** / **0.11*** / **0.11**	**0.38** / **0.39** / **0.34** / **0.37**
LSS	**0.06** / **0.05** / **0.13** / **0.08**	**0.15** / **0.10** / **0.11** / **0.12**	**0.52** / **0.54** / **0.56** / **0.54**
NSS	**0.11** / **0.09** / **0.12** / **0.11**	**0.16** / **0.13** / **0.14** / **0.14**	**0.38** / **0.45** / **0.46** / **0.43**
MLTZ-S	**0.14** / **0.08** / **0.12** / **0.11**	**0.22** / **0.14** / **0.16** / **0.17**	**0.41** / **0.32** / **0.34** / **0.36**
MLTZ-OS	**0.08** / **0.06** / **0.06** / **0.07**	**0.06** / **0.08** / **0.04** / **0.06**	**0.29** / **0.27** / **0.28** / **0.28**
NB	**0.07** / **0.05** / **0.06** / **0.06**	**0.13** / **0.04** / **0.05** / **0.08**	**0.39** / **0.30** / **0.29** / **0.33**
FC	**0.09** / **0.07** / **0.06** / **0.07**	**0.21** / **0.07** / **0.06** / **0.12**	**0.77** / **0.43** / **0.45** / **0.55**
NWC	**0.04** / **0.03** / **0.05** / **0.04**	**0.10** / **0.05** / **0.05** / **0.07**	**0.43** / **0.40** / **0.43** / **0.42**
SG	**0.03** / **0.00** / **0.06*** / **0.03**	**0.07** / **0.03** / **0.04*** / **0.04**	**0.48** / **0.46** / **0.54** / **0.49**

4.2 Variability of SST in Summer

The EOFs for the summer means are in Figure 12 and the corresponding PCs are in Figure 13. There is substantial similarity to the revised EOFs for the annual means (Figs. 5, 7), but there are also considerable differences. In particular, while the summer EOF1 modes for 1900-2011 and 1950-2011 (Fig. 12a,b) closely resemble the annual-mean EOF1 modes for these periods (Fig. 5a,b), the summer EOF2s and EOF3s for these periods are reversed from the annual-mean EOF2s and EOF3s; i.e. the summer second mode closely resembles the annual third mode, and the summer third mode closely resembles the annual second mode. Since the ordering of the modes in each case is based on the percentage of the variance explained, this just means that one mode is more important in the annual means and the other in the summer means. Comparison of the annual and summer PC2 and PC3 time series (Figs. 6 and 13) supports this interpretation.

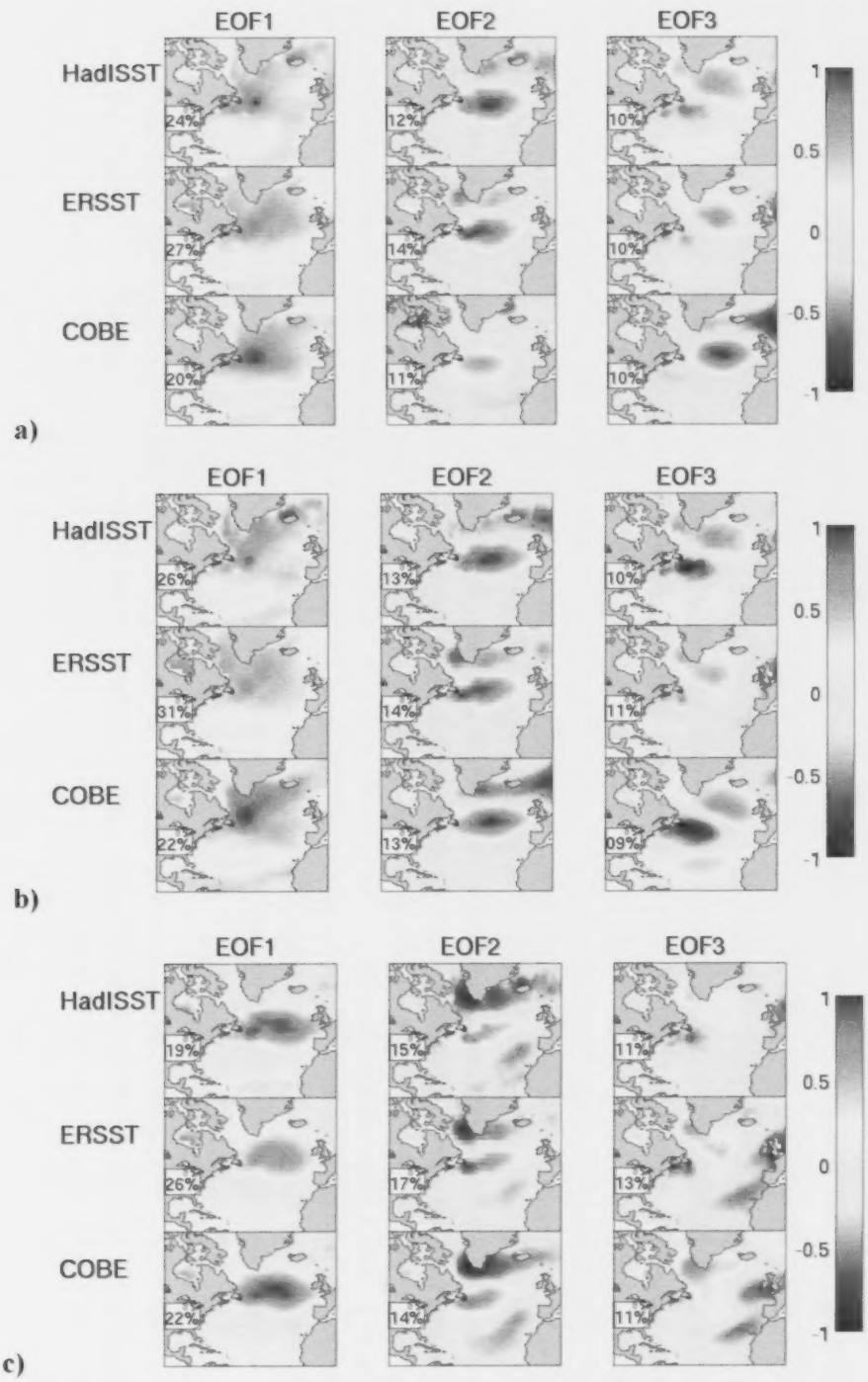

Figure 12 EOF patterns for summer means for a) 1900-2011, b) 1950-2011 and c) 1979-2011, with the percentage of variance explained in the inset panels.

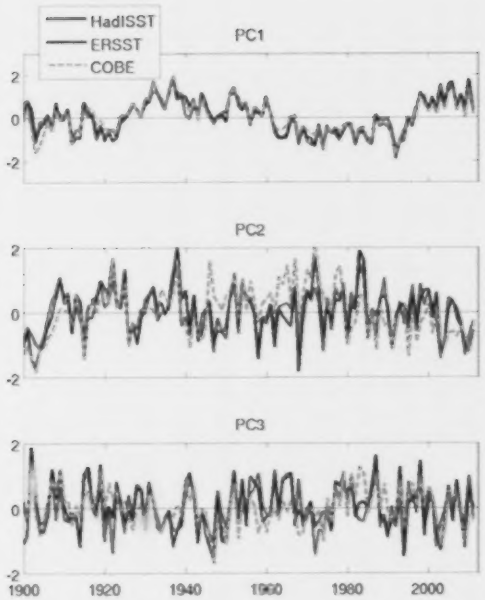

Figure 13a PCs for the summer NA analyses for 1900-2011.

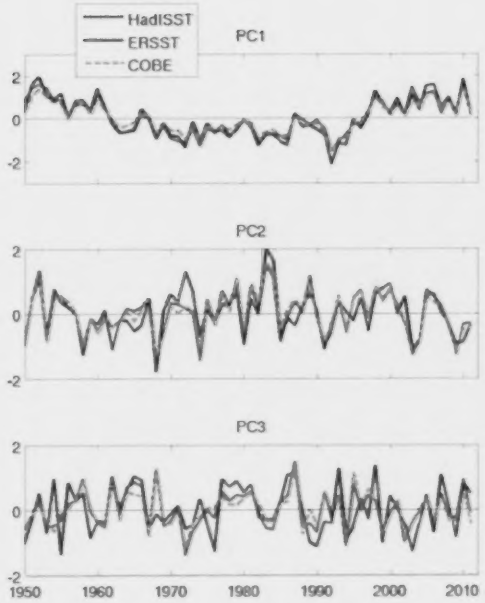

Figure 13b PCs for the summer NA analyses for 1950-2011.

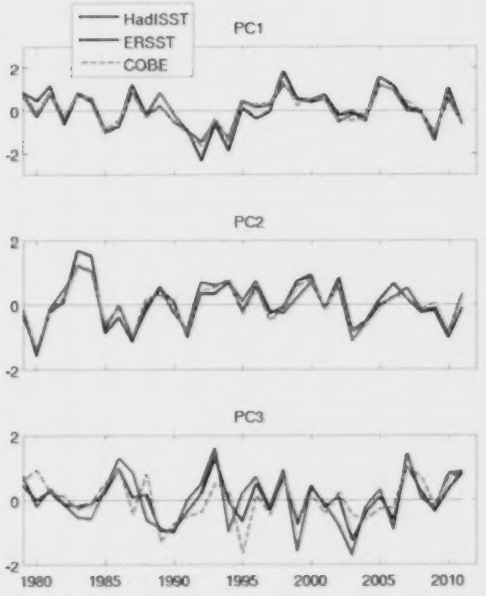

Figure 13c PCs for the summer NA analyses for 1979-2011.

The leading summer EOFs for the 1979-2011 period (Fig. 12c) are somewhat different from the leading annual-mean EOFs for this period (Figs. 5c, 7). In particular, the AMO-like first mode in the annual means is no longer present in the summer means. This is not surprising in view of the predominant multi-decadal variation in the AMO (actually, it is perhaps more surprising that this mode is as prominent as it is in the 1979-2011 annual means; closer inspection of Fig. 5c indicates that, while the spatial structure of the annual-mean EOF1 for 1979-2011 is similar to that for the longer periods, the 1979-2011 EOF1 has a spatial change in sign unlike the longer-period EOF1s). The 1979-2011 summer EOF1s (Fig. 12c) resemble the revised EOF3s for the annual means during 1900-2011 and 1950-2011 (Fig. 7) in that they have a predominant centre-of-action extending eastward from the Grand Bank in the vicinity of the North Atlantic Current and westward to the Scotian Shelf. Similarly, the 1979-2011 summer EOF2s resemble the annual-mean EOF2s for 1900-2011 (revised in Fig. 7) and 1950-2011 (Fig. 5b) in that they have a change in sign to the north of the Grand Bank (note that the signs of EOF2 and PC2 in Figs. 12c and 13c, respectively, need to be reversed in order to see this best).

Focussing on the lower-frequency variability (1900-2011 and 1950-2011), the PCs (Fig. 13a,b) confirm that the summer EOF1s are the biggest contributors, with distinct multi-decadal variations resembling the AMO-like PC1 variations in the annual means (Fig. 5a,b). The correlation coefficients between the summer PC1s and de-trended annual AMO index are 0.84, 0.86, and 0.82 for HadISST1, ERSST, and COBE, respectively. Since these values are smaller than those for the annual means, there is a suggestion that the AMO is not particularly associated with summer processes. The correlations between the summer PC2s and the de-trended winter NAO are small (magnitudes <0.1), consistent with the summer EOF2s and EOF3s being switched from their annual counterparts. The coefficients between the summer PC3s and the winter NAO are -0.30, -0.22, and -0.30, respectively, also consistent with this switch. The magnitudes of these correlations are smaller than those between the annual PC2s and winter NAO, consistent with the important role of the NAO in winter in contributing to this mode of SST variability.

Off Atlantic Canada, there are small differences among the spatial structures of the summer and annual-mean EOF1s for 1900-2011 and 1950-2011, but overall similarities. With the inclusion of the seasonal ice-covered areas off Labrador and in Baffin Bay in the summer HadISST1 domain, the broad amplified positive anomaly of EOF1 over the subpolar NA extends across the Labrador Sea to the Labrador Shelf and Baffin Bay, somewhat similar to that in ERSST and COBE. Collectively, this indicates that the AMO has been contributing to warming across the Labrador Sea and as far north as Davis Strait during the past two decades, suggesting that the warming trend seen in recent decades in DFO observations and in the 1979-2011 SST trends (Figs. 4 and 11) may include a contribution from natural variability.

Section 5 SST Variability at DFO Monitoring Sites

5.1 Comparison of Gridded SST with DFO Observations

In this subsection, we compare time series of annual mean upper-ocean temperature from DFO monitoring sites with time series constructed by interpolating the gridded data to positions near these sites. The time series for the entire length of the DFO records and from the gridded data are shown in Figure 14. Some similarities are expected because some of the observations contributing to the DFO time series probably also contribute to the gridded historical datasets. Some differences are expected from factors such as differing source data, possible differing criteria for "surface" in the datasets, limited winter data at Bravo, and the location of the Prince 5 site in a coastal estuary.

There are substantial similarities among the time series from the gridded historical datasets, and between them and the DFO time series, at all sites. In particular, there is similar inter-annual to multi-decadal variability among the time series at Prince 5, even though the temperatures in the DFO time series are lower (as expected) than those in the gridded datasets by ~2°C. There is similar multi-year to multi-decadal variability among the historical and DFO time series from Emerald Basin and Station 27, even though the means and inter-annual variations differ in some cases. There is also general similarity among the time series for Bravo, particularly on decadal and multi-decadal time scales, even though the DFO time series does not capture some of the multi-year features that are common to two or more of the gridded datasets (and, vice-versa, the gridded datasets do not show some of the interannual variability in the DFO time series).

The HadISST1 values are noticeably higher than the ERSST and COBE ones since about 1970 at Prince 5 and Emerald Basin, over the entire record (since 1948) at Station 27, and before 1975 at Bravo. Similarly, the ERSST values are noticeably lower than the other gridded datasets since 1985 at Station 27 and over the entire record at Bravo. These variations raise the possibility of a systematic difference in the sampling or underlying data, or in the temperature structure (e.g. spatial gradients), during some periods and at some sites. This might help explain the differences in the trends among the different gridded datasets in Figures 4 and 11.

The trends in the various datasets during the DFO data periods in Figure 14 are presented in Table 4. The DFO time series have statistically significant trends of 0.1°C/decade at Prince 5 and Station 27, a near-significant ($p = 0.11$) trend of 0.081°C/decade at Emerald Basin, and no significant trend at Bravo (note that these are over different periods, so their differences reflect a mixture of spatial and temporal variability; also the statistical significance may be overestimated due to auto-correlation in the time series). While the differences among the trends from the different historical datasets are generally qualitatively similar to those among the trends for the corresponding regions in Table 2, there are large quantitative differences with the site-specific trends (Table 4) showing wider variability among datasets at all sites except Station 27. This points to the importance to local applications of the small-scale spatial structure in the trends apparent in Figures 4 and 11. On the positive side, the trends from the DFO data are within the

range (and near the average) of the trends from the three historical datasets at three of the sites (but not at Bravo).

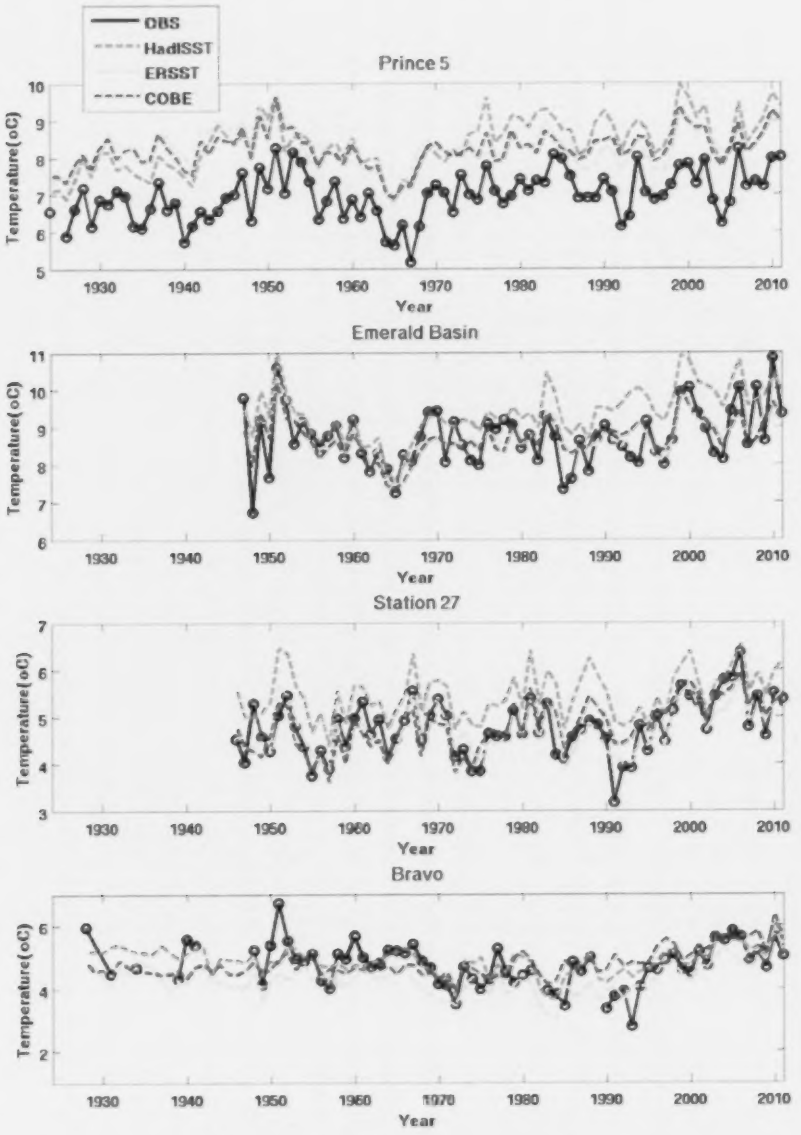

Figure 14 Time series of annual means of surface temperature at four DFO monitoring sites (black), and of SST in the vicinity of the sites from the three gridded historical datasets (coloured lines). See Section 2.1 for information on the DFO time series.

Table 4 Trends in annual-mean upper-ocean temperature (°C/decade) over the entire period of record at the DFO monitoring sites, together with the trends in the annual-mean SST datasets at nearby positions (i.e. of the time series shown in Fig. 14) and the average of the trends (Avg Hist) for these historical datasets. Trends significant at the 95% confidence level (without consideration of autocorrelation in the time series) are in **boldface**.

Station	Period	DFO	HadISST1	ERSST	COBE	Avg Hist
Prince 5	1924-2011	**0.10**	**0.16**	0.02	**0.05**	0.08
Emerald Basin	1947-2011	0.08	**0.18**	0.05	**0.09**	0.11
Station 27	1946-2011	**0.10**	**0.07**	**0.08**	**0.17**	0.08
Bravo	1908-2011	-0.004	0.003	**0.05**	**0.12**	0.06

5.2 Contributions of Basin-Scale Modes to SST Variations at DFO Monitoring Sites

The contributions of the primary EOF modes at specific geographic locations can be computed by multiplying the PC time series (e.g. Fig. 6) for that mode by the EOF amplitude (e.g. Fig. 5) at each location. This is particularly useful for the EOF modes that are associated with known large-scale SST variation patterns; for example, EOF1 corresponding to the AMO, and EOF2 including a contribution from NAO forcing. The resulting time series indicate the contribution of the large-scale patterns to local variability. This contribution from natural climate variability can then be considered in identifying whether apparent short-term trends at particular locations are related to natural modes of variability or to anthropogenic climate changes.

The DFO monitoring time series and the contributions of the AMO (first mode) from the NWA analyses of the gridded datasets are shown in Figure 15. The same DFO observations and the contributions from the NAO-linked second mode are shown in Figure 16. Correlation coefficients between the observed and modal time series at each site are in Table 5.

It is clear from the time series (Fig. 15) and the correlations (Table 5) that the AMO (first mode) makes a major contribution to the low-frequency (decadal and multi-decadal) variability at Bravo, and a substantial (~40%) contribution to the total variance in the annual means at Bravo. In contrast, the contribution of the AMO to the overall variability at the other sites is much smaller (<2% of the variance) and not statistically significant. There is a hint of an AMO contribution to the low-frequency variability at Station 27 and at Emerald Basin, even though it contributes to only a small fraction of the variance in the time series of annual means. The range of the multi-decadal AMO variations at the sites varies from ~1°C at Bravo to ~0.5°C at Station 27 and ~0.1-0.2°C in Emerald Basin and at Prince 5. There is approximate consistency among the AMO contributions from the different datasets at the Bravo, Station 27, and Emerald Basin sites, but the differences are comparable to the range of the AMO variation at Prince 5.

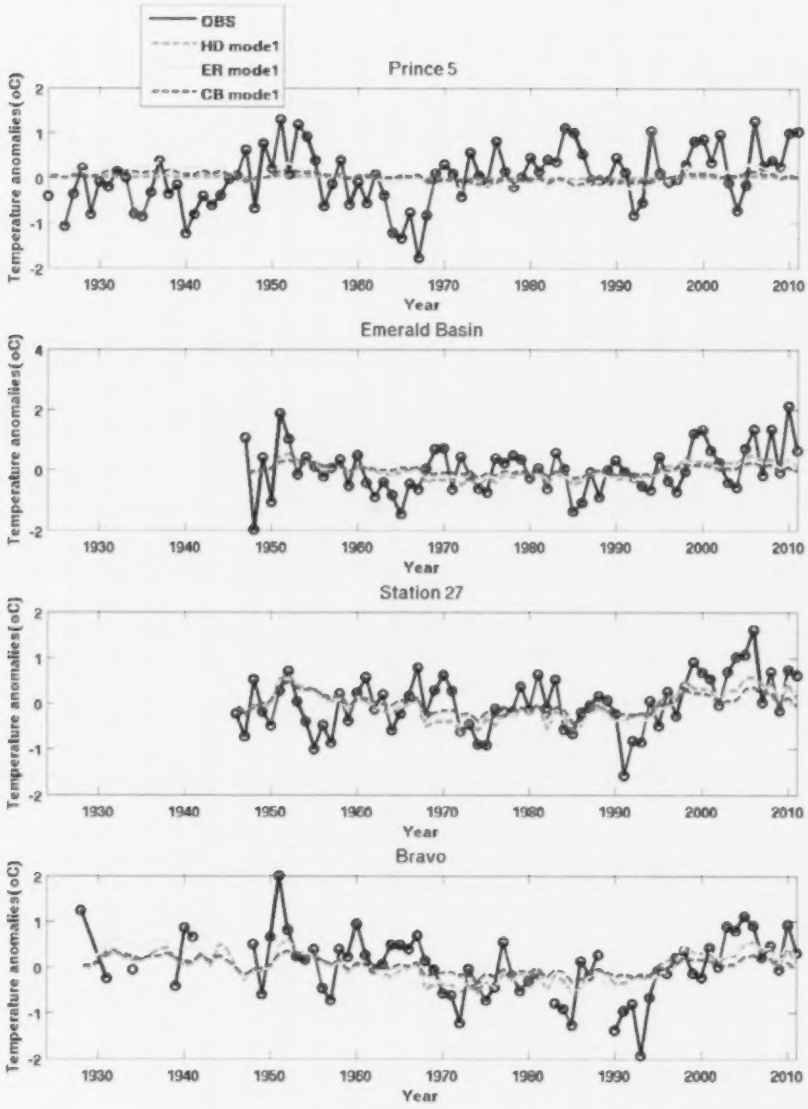

Figure 15 Observed annual-mean anomalies of surface temperature (black circles connected by lines) at the four DFO monitoring sites together with the contributions to local SST variability from the AMO in the three gridded datasets (coloured lines). The AMO contributions are taken from the first mode of the EOF analysis of the de-trended annual means over the NWA during 1900-2011. HD refers to HadISST1, ER to ERSST and CB to COBE.

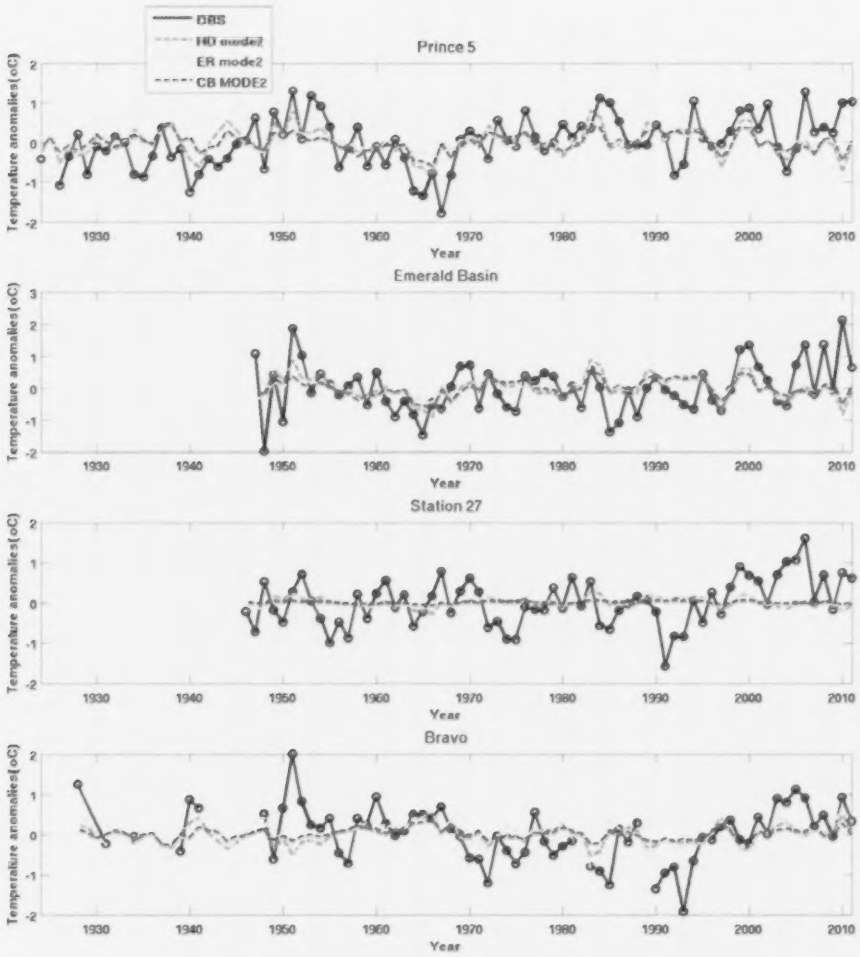

Figure 16 Observed annual mean anomalies of surface temperature (black circles and lines) at the four DFO monitoring sites together with the contributions to historical SST variability from the NAO-linked mode 2 in the three gridded datasets (coloured lines; same abbreviated acronyms as in Figure 15). The second mode is from the EOF analysis of the de-trended annual means over the NWA during 1900-2011, with the revised second mode used for COBE.

The NAO-linked second mode in all three datasets makes significant contributions to SST variability at Bravo (14-18% of the variance) and Prince 5 (8-18% of variance), but smaller contributions (1-6% of variance) at Emerald Basin and Station 27 (Fig. 16, Table 5). The contributions at Prince 5 and Emerald Basin have the opposite phase to those at Bravo and Station 27, as expected from the spatial structure of the revised EOF2s in Figs. 5, 7, and 9. This mode contributes more broadly (but weakly) to variability on various time scales (multi-decadal to inter-annual) than the AMO-like mode.

Table 5 Correlation coefficients between the observed upper-ocean annual temperature anomalies from DFO monitoring at four sites in the NWA, and the contributions of the first (AMO-like; left columns), second (NAO-linked; middle columns) and third (right columns) modes from the EOF analyses of the three gridded historical datasets for the NWA domain and the period 1900-2011. Both the DFO and historical dataset indices were de-trended before the computations. Coefficients that are statistically significant at the 95% level are indicated in **boldface**. The datasets are indicated by the abbreviated acronyms HD (HadISST1), ER (ERSST) and CB (COBE).

Station	PC1 (AMO-like)			PC2 (NAO-linked)			PC3 (ocean gyres)		
	HD	ER	CB	HD	ER	CB	HD	ER	CB
Prince 5	0.12	0.13	0.09	**0.43**	**0.28**	**0.35**	**0.33**	**0.47**	**0.30**
Emerald Basin	0.06	0.05	0.08	0.17	0.12	0.14	0.03	-0.004	-0.07
Station 27	-0.12	-0.09	-0.14	0.20	0.10	0.23	-0.19	**-0.33**	-0.18
Bravo	**0.64**	**0.67**	**0.58**	**0.38**	**0.40**	**0.42**	0.17	0.08	**0.26**

The correlation coefficients between the PC3s and the DFO annual anomalies (Table 5) indicate a significant contribution (9-22% of the variance) from the third mode in all three datasets to observed variability at Prince 5, smaller contributions at Station 27 (3-11%) and Bravo (1-7%), and no contribution at Emerald Basin. The contributions at Prince 5 are shown in Figure 17, indicating that this mode contributes in particular to the warmer SSTs in the Gulf of Maine region in the early 1950s and cooler SSTs in the 1960s (particularly for COBE). This mode is, thus, an additional factor (to the second mode) in the cooler SSTs observed west of the Grand Bank in the 1960s (Petrie and Drinkwater, 1993), with the present results indicating that it contributes more in the Gulf of Maine and the second mode contributes more on the Scotian Shelf.

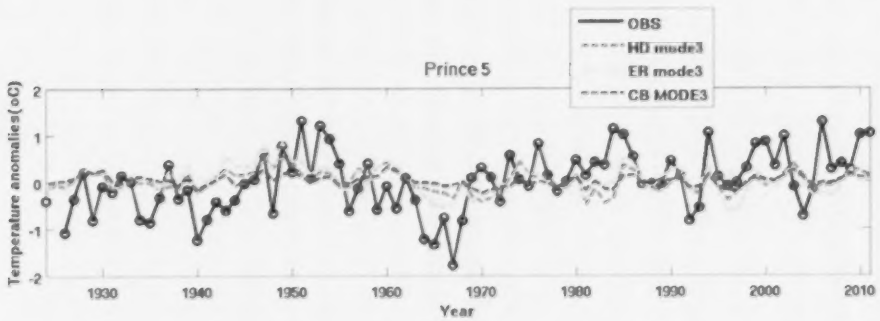

Figure 17 Observed annual mean anomalies of surface temperature (black circles and lines) at Prince 5 together with the contributions to historical SST variability from the third mode in the three gridded datasets (coloured lines; same abbreviated acronyms as in Table 5). The third mode is from the EOF analysis of the de-trended annual means over the NWA during 1900-2011, with the revised third mode used for COBE.

To conclude the comparison between the historical datasets and time series from monitoring, several comments are appropriate. First, large-scale modes contribute to regional SST variability as expected. Second, it appears that multiple modes contribute to the variability at some sites, even on similar time scales. Third, a large portion of the local variability in annual time series, particularly at high frequencies (e.g. inter-annual) cannot be explained by the leading modes examined here. Corollaries of this are that the large-scale modes are more important to multi-year and lower-frequency variability than indicated by the percentages of explained variance, and forcings such as the NAO may make additional contributions to local variability through modes not examined here (or through local effects).

Section 6 Summary

Common trend and EOF analyses for the NA were carried out using three different global historical gridded (interpolated) datasets of monthly SST: HadISST1, ERSST and COBE. Analyses have been carried out for three periods (1900-2011, 1950-2011, 1979-2011), and for annual (over 12 months) and summer (Jul-Aug-Sept) means. Analyses have also been carried out for a smaller NWA domain for annual means from 1900-2011. Time series from the historical datasets were compared with observations from DFO monitoring programs at four sites off Atlantic Canada.

While there are many similarities in the results from the different gridded datasets, there are also notable differences that are probably related to data sparsity in some areas and different methods, interpolations, corrections and sources of the data. In particular, there is a clear indication that the magnitudes and spatial structure of the long-term (1900-2011 and 1950-2011) trends from these datasets need to be used and interpreted with caution. The comparisons with the DFO time series indicate qualitative similarities in the trends and variability among the gridded and monitoring datasets at all four sites, but also notable quantitative differences.

There is a particular data quality issue for the COBE SSTs immediately adjacent to the Greenland coast, apparently associated with suspect changes in the 1970s. This manifests as anomalous long-term warming during 1900-2011 and 1950-2011, a spurious second mode in the EOF analysis for 1900-2011, and a spurious third mode for 1950-2011. If these modes are ignored in the comparisons, then there is good agreement across the three datasets for the first three modes (see below).

For 1900-2011, there is warming of 0.05 to 0.1°C/decade over most of the NA (excluding coastal waters off Greenland) in the annual means from all three datasets, but an area of cooling or reduced warming south of Greenland and extending into the off-shelf waters off Labrador and Newfoundland. There is warming on the Atlantic Canadian shelf/slope in all the datasets but differences in the pattern of its magnitude (0.01 to 0.1°C/decade). The COBE data have the largest differences among the datasets. Differences in the trends between the Labrador Sea and Scotian Shelf previously identified in the HadISST1 data (Loder et al., 2012) are not present in ERSST and COBE data. For 1950-2011 and 1979-2011, there is greater similarity in the pattern of the trends from the different datasets but still significant differences off Atlantic Canada. Average (across datasets) trends in the annual means for Atlantic Canadian shelf/slope regions are 0.08 to 0.13°C/decade for 1950-2011 and 0.2 to 0.5°C/decade for 1979-2011 (where the range reflects spatial variability). Summer trends are generally larger than annual-mean trends, but not in all parts of the Atlantic Canadian shelf/slope.

The most robust results for 1900-2011 (and 1950-2011) are the remarkable similarity of the first EOF mode in the three annual-mean datasets and the predominance of a multi-decadal variation with a range of about 2°C in the PC time series. This closely resembles the AMO (e.g. Wang et

al., 2012). This EOF accounts for 31-41% of the variance in the annual means for the NWA and has a widespread SST variation over the NA. However, there is a large difference in amplitude between its maximum in the subpolar gyre (and extending weakly west of the Grand Bank) and its minimum in the subtropical gyre in the western NA. Implications are that the influence of the AMO is greater east of the Grand Bank than to its west, and that the AMO contributed significantly to the amplified warming in the subpolar NWA during the past three decades. The contributions of the first EOF at the DFO sites indicate that the AMO is a major factor in the multi-decadal variability at Bravo, but only a secondary one in the decadal to multi-decadal variability at the other sites.

The pattern of the second EOF in the annual means (after exclusion of the original spurious COBE mode), during 1900-2011, is also similar across the three datasets, accounting for 11-16% of the variance in the NWA. It resembles the out-of-phase changes in upper-ocean temperature north and west of the Grand Bank described by Petrie and Drinkwater (1993) and Deser et al. (2010), and attributed to the NAO. The PC2s for 1900-2011 are modestly correlated (coefficient magnitudes: $r \sim 0.5$) with the winter NAO index, such that we have referred to this mode as NAO-linked. The local contributions of this mode are modestly correlated ($r \sim 0.4$) with the DFO time series from Bravo and Prince 5 but, somewhat surprisingly, not significantly correlated with the series for Station 27 and Emerald Basin ($r \sim 0.1$-0.2). The low coefficients may be partly due to the strong inter-annual variability at the various sites, such that an analysis of the time series after low-pass filtering would show a much greater NAO influence.

The EOFs and PCs for the third mode in the annual means for 1900-2011 are also similar across the three datasets, accounting for 7-12% of the variance in the NWA. This EOF has a prominent centre-of action near the North Atlantic Current extending eastward from the Grand Bank, and an opposite phase in and to the south of the Gulf of Maine. It contributes significantly ($r \sim 0.3$-0.5) to the DFO-observed variability at Prince 5. Its PCs are weakly to moderately correlated with the sea level difference between Bermuda and Bravo ($r \sim 0.2$-0.4) in a hindcast simulation of NA circulation during 1958-2004 (Wang et al., 2013), and with the observed curl of the wind stress over the NA ($r \sim 0.3$-0.5) during this period. This suggests that this third mode could be related to variability in ocean circulation and to interactions between the subpolar and subtropical gyres in particular. However, further investigation of this, and the first two and other modes, is needed to clarify the origins and implications.

The pattern and amplitudes of the summer EOF1s in the open NA are similar to those for the annual-mean EOF1s for all three datasets during 1900-2011 and 1950-2011, and the corresponding PC1s are similar across the datasets and periods. The PC1 correlations with the AMO are lower for the summer means ($r \sim 0.84$) than the annual means ($r > 0.9$) indicating that, while summer SST variability in the NA includes a significant AMO-like component, the AMO may originate primarily in other seasons. The summer analysis of HadISST1 indicates that the enhanced AMO signal in the subpolar region extends across the Labrador Sea to the Labrador coast.

The EOF2s and EOF3s, and the PC2s and PC3s, for the summer means are similar to those for the annual means during 1900-2011 and 1950-2011, but their order is switched with respect to the percentage of total explained variance for the NA. For example, the NAO-linked mode ranks second in percentage variance explained in the annual means (10-14% compared to 7-10% for the circulation-linked mode during 1900-2011), but third in variance explained in the summer means (10% compared to 11-14% for the circulation mode). Since these differences are small, the main point is that the NAO- and circulation-linked modes are similar in the annual and summer means.

In conclusion, it should be stated that, while our results should help place upper-ocean temperature variability in the Atlantic LAB off Canada in a NA-wide and broader climate variability perspective, many questions and issues remain regarding the space-time scales and origins of the apparent natural variability, and the magnitudes and spatial patterns of anthropogenic changes. Further analyses with observational and model data for other ocean and climate variables are needed.

Acknowledgements

This work was carried out with support from the Atlantic Trends and Projections activity of DFO's Aquatic Climate Change Adaptation Services Program (ACCASP). We are grateful to the organizations that developed the three gridded SST datasets used in the report. We are also grateful to Eugene Colbourne and Igor Yashayaev who made the DFO monitoring time series available, and to others who contributed to them. Finally, we thank Ingrid Peterson, Guoqi Han, Dave Brickman, and others who provided helpful input during discussions and internal review.

References

Belkin, I. 2009. Rapid warming of large marine ecosystems. *Prog. Oceanogr.* 81, 207-213.

Brock, R.J., E. Kenchington and A. Martinez-Arroyo (Eds.). 2012. Scientific guidelines for designing resilient marine protected area networks in a changing climate. Commission for Environmental Cooperation. Montreal, Canada, 95 p. http://www3.cec.org/islandora/en/item/10820-scientific-guidelines-designing-resilient-marine-protected-area-networks-in-changing-en

Chylek, P., C. Folland, L. Frankcombe, H. Dijkstra, G. Lesins and M. Dubey. 2012. Greenland ice core evidence for spatial and temporal variability of the Atlantic Multidecadal Oscillation. *Geophys. Res. Lett.* 39, L09705, doi:10.1029/2012GL051241

Colbourne, E., J. Craig, C. Fitzpatrick, D. Senciall, P. Stead and W. Bailey. 2012. An assessment of the physical oceanographic environment on the Newfoundland and Labrador Shelf during 2011. DFO Can. Sci. Advis. Sec. Res. Doc. 2012/044: iv + 32 p. http://www.dfo-mpo.gc.ca/csas-sccs/Publications/ResDocs-DocRech/2012/2012_044-eng.pdf

Deser, C., M.A. Alexander, S.-P. Xie and A.S. Phillips. 2010. Sea surface temperature variability: patterns and mechanisms. *Ann. Rev. Mar. Sci.* 2, 115-143.

Drijfhout, S., G.J. van Oldenborgh and A. Cimatoribus. 2012. Is a decline of AMOC causing the warming hole above the North Atlantic in observed and modeled warming patterns? *J. Clim.* 25, 8373-8379.

Friedland, K.D., and J. A. Hare. 2007. Long-term trends and regime shifts in sea surface temperature on the continental shelf of the northeast United States. *Cont. Shelf Res.* 27, 2313–2328.

Galbraith, P.S. and P. Larouche. 2013. Trends and variability in eastern Canada sea-surface temperatures. Ch. 1 (p. 1-18) *In:* Aspects of climate change in the Northwest Atlantic off Canada [Loder, J.W., G. Han, P.S. Galbraith, J. Chassé and A. van der Baaren (Eds.)]. Can. Tech. Rep. Fish. Aquat. Sci. 3045: x + 192 p.

Hakkinen, S., P.B. Rhines and D.L. Worthen. 2011. Atmospheric blocking and Atlantic Multidecadal ocean variability. *Science* 334, 655-659.

Han, G., Z. Ma and H. Bao. 2013. Trends of temperature, salinity, stratification and mixed-layer depth in the Northwest Atlantic. Ch. 2 (p. 19-32) *In:* Aspects of climate change in the Northwest Atlantic off Canada [Loder, J.W., G. Han, P.S. Galbraith, J. Chassé and A. van der Baaren (Eds.)]. Can. Tech. Rep. Fish. Aquat. Sci. 3045: x + 192 p.

Hebert, D. 2013. Trends in temperature, salinity, density and stratification for different regions in the Atlantic Canadian shelf. Ch.3 (p. 33-42) *In:* Aspects of climate change in the Northwest Atlantic off Canada [Loder, J.W., G. Han, P.S. Galbraith, J. Chassé and A. van der Baaren (Eds.)]. Can. Tech. Rep. Fish. Aquat. Sci. 3045: x + 200 p.

Hebert, D., R. Pettipas, B. Petrie and D. Brickman. 2012. Meteorological, sea ice and physical oceanographic conditions on the Scotian Shelf and in the Gulf of Maine during 2011. DFO Can. Sci. Advis. Sec. Res. Doc. 2012/055: vi + 43 p. http://www.dfo-mpo.gc.ca/Csas-sccs/publications/resdocs-docrech/2012/2012_055-eng.pdf

Ishii, M., M. Kimoto, K. Sakamoto, and S. Iwasaki. 2006. Steric sea level changes estimated from historical ocean subsurface temperature and salinity analyses. *J. Oceanogr.* 62, 155-170,

Ishii, M., A. Shouji, S. Sugimoto and T. Matsumoto. 2005. Objective analyses of sea-surface temperature and marine meteorological variables for the 20th century using COADS and the KOBE collection. *Intern. J. Climatol.* 25, 865-869.

Knight, J.R., R.J. Allan, C. Folland, M. Vellinga and M.E. Mann. 2005. A signature of persistent natural thermohaline cycles in observed climate. *Geophys. Res. Lett.* 32, L20708, doi:10.1029/2005GL024233.

Knudsen, M.F., M.-S. Seidenkrantz, B.H. Jacobsen and A. Kuijers. 2013. Tracking the Atlantic Multidecadal Oscillation through the last 8,000 years. *Nature Communications* 2, 178, doi:10.1038/ncomms1186

Loder, J.W., J. Chasse, P. Galbraith, G. Han, D. Lavoie and others. 2013. Summary of climate change trends and projections for the Atlantic Large Aquatic Basin off Canada. Can Tech Rep Fish Aquat Sci. 3051 (under revision).

Loder, J.W., A. van der Baaren, E. Colbourne, G. Han, D. Hebert, B. Merryfield, I. Peterson and I. Yashayaev. 2012. Challenges in projecting ocean climate change in the NW Atlantic. 46th Annual CMOS Congress, Montreal, Canada. https://www1.cmos.ca/abstracts/abstract_print_view.asp?absId=5606

Medhaug, I. and T. Furevik. 2011. North Atlantic 20th century multidecadal variability in coupled climate models: sea surface temperature and ocean overturning circulation. *Ocean. Sci.* 7, 389-404.

O'Brien, T.D., W.K.W. Li and X.A.G. Morán [Eds.] 2012. ICES phytoplankton and microbial plankton status report 2009/2010. ICES Cooperative Research Report No. 313 http://www.ices.dk/sites/pub/Publication%20Reports/Cooperative%20Research%20Report%20(CRR)/crr313/ICES%20313%20-WEB.pdf

Ou, H.-W. 2012. A minimal model of the Atlantic Multidecadal Variability. *Clim. Dyn.* 38, 775-794.

Park, W., and M. Latif. 2010. Pacific and Atlantic multidecadal variability in the Kiel climate model. *Geophys. Res. Lett.* 37, L24702, doi:10.1029/2010GL045560.

Petrie, B., and Drinkwater, K.D. 1993. Temperature and salinity variability on the Scotian Shelf and Gulf of Maine 1945-1990. *J. Geophys. Res.* 98, 20079-20089.

Petrie, B. 2007. Does the North Atlantic Oscillation affect hydrographic properties on the Canadian Atlantic continental shelf? *Atmos.-Ocean* 45, 141–151.

Polyakov, I.V., V.A. Alexeev, U.S. Bhatt, E.I. Polyakov and X. Zhang. 2010. North Atlantic warming: patterns of long-term trend and multidecadal variability. *Clim. Dyn.* 34, 439-457.

Rayner, N.A., A. Kaplan, E.C.Kent, R.W. Reynolds, P. Brohan, K.S. Casey, J.J. Kennedy, S.D. Woodruff, T.M. Smith, C. Donlon, L.-A. Breivik, S. Eastwood, M. Ishii and T. Brandon. 2010. Evaluating climate variability and change from modern and historical SST observations. p. 819-829 *In:* Proceedings of the OceanObs '09 Conference, Vol. 2.2 – Community White

Papers (Part 2), Eds. J. Hall, D.E. Harrison and D. Stammer, European Space Agency WPP-306. http://www.oceanobs09.net/proceedings/

Rayner, N.A., D.E. Parker, E.B. Horton, C.K.Folland, L.V. Alexander, D.P. Rowell, E.C. Kent and A. Kaplan. 2003. Global analyses of sea surface temperature, sea ice, and night marine air temperature since the late nineteenth century. *J. Geophys. Res.* 108 (D14), 4407, doi:10.1029/2002JD002670.

Robson, J., R. Sutton, K. Lohmann, D. Smith, and M. D. Palmer. 2012. Causes of the rapid warming of the North Atlantic ocean in the mid 1990s, *J. Clim.*, 25, 4116–4134.

Shearman, R.K., and S.J. Lentz. 2010. Long-term sea surface temperature variability along the U.S. east coast. *J. Phys. Oceanogr.* 40, 1004–1017.

Smith, T.M., R.W. Reynolds, T.C. Peterson and L. Lawrimore. 2008. Improvements to NOAA's historical merged land-ocean surface temperature analysis (1880-2006*)*, *J. Clim.* 21, 2283-2296.

Terray, L. 2012 Evidence for multiple drivers of North Atlantic multi-decadal climate variability. *Geophys. Res. Lett.* 39, L19712, doi:10.1029/2012GL053046

Wang, C., S. Dong, A.T. Evan, G.R. Foltz and S.-K. Lee. 2012. Multidecadal covariability of North Atlantic sea surface temperature, African dust, Sahel rainfall, and Atlantic hurricanes. *J. Clim.* 25, 5404-5425.

Wang, Z., Y. Lu, F. Dupont, J.W. Loder, C. Hannah and D.G. Wright. 2013. Variability of sea surface height and circulation in the North Atlantic: forcing mechanisms and linkages. *Progr. Oceanogr.* (in press)

Wu, L., W. Cai, L. Zhang, H. Nakamura, A. Timmerman, T. Joyce, M.J. McPhaden, M. Alexander, B. Qoi, M. Visbeck, P. Chang and B. Giese. 2012. Enhanced warming over the global subtropical western boundary currents. *Nature Clim. Change* 2, 161-166.

Yashayaev, I. 2007. Hydrographic changes in the Labrador sea, 1960-2005. *Progr. Oceanogr.* 73 (3-4), 242-276.

Yashayaev, I, and B. Greenan. 2012. Environmental conditions in the Labrador Sea during 2011. Northwest Atlantic Fisheries Organization Scientific Research Document 12/018, N6042, 17 pp. http://archive.nafo.int/open/sc/2012/scr12-018.pdf

Yasunaka, A.S., and K. Hanawa. 2011. Intercomparison of historical sea surface temperature datasets. *Int. J. Climatol.* 31, 1056-1073.

Yu, B., and G.J. Boer, 2006. The variance of sea surface temperature and projected changes with global warming. *Clim. Dyn.* 26, 801–821.